The Journal of Neuroscience, June 15, 2000, 20(12):4582–4595

Potentiation of NMDA Receptor Function by the Serine Protease Thrombin

Melissa B. Gingrich, Candice E. Junge, Polina Lyuboslavsky, and Stephen F. Traynelis

Department of Pharmacology, Emory University School of Medicine, Atlanta, Georgia 30322

Although serine proteases and their receptors are best known for their role in blood coagulation and fibrinolysis, the CNS expresses many components of an extracellular protease signaling system including the protease-activated receptor-1 (PAR1), for which thrombin is the most effective activator. In this report we show that activation of PAR1 potentiates hippocampal NMDA receptor responses in CA1 pyramidal cells by 2.07 ± 0.27-fold (mean ± SEM). Potentiation of neuronal NMDA receptor responses by thrombin can be blocked by thrombin and a protein kinase inhibitor, and the effects of thrombin can be mimicked by a peptide agonist (SFLLRN) that activates PAR1. Potentiation of the NMDA receptor by thrombin in hippocampal neurons is significantly attenuated in mice lacking PAR1. Although high concentrations of thrombin can directly cleave both native and recombinant NR1 subunits, the thrombin-induced potentiation we observe is independent of NMDA receptor cleavage. Activation of recombinant PAR1 also potentiates recombinant NR1/NR2A (1.7 ± 0.06-fold) and NR1/NR2B (1.41 ± 0.11-fold) receptor function but not NR1/NR2C or NR1/NR2D receptor responses. PAR1-mediated potentiation of recombinant NR1/NR2A receptors occurred after activation with as little as 300 pM thrombin. These data raise the intriguing possibility that potentiation of neuronal NMDA receptor function after entry of thrombin or other serine proteases into brain parenchyma during intracerebral hemorrhage or extravasation of plasma proteins during blood–brain barrier breakdown may exacerbate glutamate-mediated cell death and possibly participate in post-traumatic seizure. Furthermore, the ability of neuronal protease signaling to control NMDA receptor function may also have roles in normal brain development.

Key words: serine protease; thrombin; NMDA receptor; protease receptor; PAR1; hippocampal neurons

It is becoming increasingly apparent that the CNS expresses many serine proteases and zymogen precursors, as well as unique members of the serpin class of selective serine protease inhibitors (Nakajima et al., 1992; Sumi et al., 1992; Chen et al., 1995; Gschwend et al., 1997; Hastings et al., 1997; Krueger et al., 1997; Luthi et al., 1997; Pindon et al., 1997; Scarisbrick et al., 1997; Shimizu et al., 1998; Yamamoto and Loskutoff, 1998). The G-protein-coupled thrombin receptor protease-activated receptor-1 (PAR1) is also present in the developing and mature CNS, with expression in specific cells such as the CA1 pyramidal neurons of the hippocampus (Weinstein et al., 1995; Niclou et al., 1998). Although endogenous activators for this receptor in the brain have not been defined, the mRNA for the thrombin precursor prothrombin and the protein that converts prothrombin to thrombin (Factor Xa) are both expressed in CNS tissue (Dihanich et al., 1991, Yamada and Nagai, 1996). In addition, blood-derived thrombin and other PAR1 activators such as plasmin will directly enter brain tissue during penetrating head wound, hemorrhagic stroke, rupture of cerebral aneurysms or arteriovenous malformations, and possibly therapeutic treatment with tissue plasminogen activator (tPA). Furthermore, if thrombin (36.7 kDa) is generated in sufficient quantities during occlusive stroke or other insults that increase blood–brain barrier permeability, it would be expected to penetrate brain parenchyma given the permeability of larger molecular weight markers such as albumin (66 kDa) (Laursen et al., 1993) and dextran (71 kDa) (Du et al., 1996). Some blood-derived serine proteases can directly increase blood–brain barrier permeability (Nagy et al., 1998). The total quantity of active thrombin that can be produced from blood is 260–360 U/ml (Seegers, 1962; Arand and Sawaya, 1986), suggesting that prothrombin circulates at high concentrations (>1 μM). Plasminogen circulates in blood at ~2 μM (Majerus et al., 1996).

The possibility that thrombin and other blood proteases might enter brain tissue under pathological conditions raises the potential for aberrant activation of protease receptors with potentially detrimental consequences. This possibility is supported indirectly by several observations. Thrombin infusion into rat caudate nucleus can produce a glial scar similar to that typical of traumatic head injury (Nishino et al., 1993; Motohashi et al., 1997). Furthermore, thrombin activation of PAR1 triggers neurite retraction, glial proliferation, and apoptosis (Gurwitz and Cunningham, 1988; Cavanaugh et al., 1990; Grabham and Cunningham, 1995; Donovan et al., 1997). Thrombin directly injected into the rat basal ganglia causes edema and precipitates seizures (Lee et al., 1996, 1997), suggesting that thrombin, in addition to heme-derived iron, may contribute to post-traumatic seizures (Willmore et al., 1978). The best indicators of post-traumatic epilepsy—subdural hematoma and intracerebral hemorrhage (Willmore 1990; Lee and Lui, 1992; Annegers et al., 1998)—could both

Received Jan. 18, 2000; revised March 28,2000; accepted April 7, 2000.

This work was supported by the National Institute of Mental Health (M.B.G.), and the National Institute of Neurological Diseases and Stroke (S.F.T.), The John Merck Fund (S.F.T.), and the Emory University Research Committee (S.F.T.). We thank Dr. R. Dingledine for critical comments on this manuscript, and D. Falls, D. Wigston, and A. Levey for helpful comments during the course of this project. We thank Drs. S. Coughlin, A. Levey, S. Heinemann, R. Huganir, S. Nakanishi, and P. Seeburg for sharing molecular reagents with us. We also thank Drs. J. Conn, J. Doherty, A. Levey, M. Marino, S. Rouse, and E. Marchan for help with some of these experiments, Dr. F. Jaramillo for help with imaging experiments, Dr. M. Hollmann for advice on isolated oocyte membranes, and N. Ciliax, N. Patel, and J. Therien for excellent technical assistance.

Correspondence should be addressed to Dr. Stephen Traynelis, Department of Pharmacology, 5025 Rollins Research Center, 1510 Clifton Road, Atlanta, GA 30322-3090. E-mail: strayne@emory.edu.

potentially lead to entry of serine proteases such as thrombin from the vasculature into the brain.

In this study we have evaluated the possibility that thrombin actions on PAR1 might modify NMDA receptor function, which is an important contributor to both seizure initiation and neurodegeneration subsequent to cerebrovascular insult or traumatic brain injury (Bradford 1995; Whetsell, 1996; Obrenovitch and Urenjak, 1997; Dirnagl et al., 1999; Lee et al., 1999).

Some of these results have been published previously in abstract form (Butler and Traynelis, 1996; Gingrich et al., 1997, 1998; Gingrich and Traynelis, 1998; Junge et al., 1999).

MATERIALS AND METHODS

Electrophysiological recording from rat and mouse hippocampal slices. Mice or rats [postnatal day 12–21 (P12–P21)] were anesthetized using isoflurane and decapitated, and the hippocampus was rapidly dissected. All procedures involving animals have been approved by the Emory University Institutional Animal Care and Use Committee. Transverse hippocampal slices (250–300 μm) were cut in ice-cold artificial CSF (ACSF) using a vibratome and secured in a submerged recording chamber perfused with 1 μM tetrodotoxin and 10 μM bicuculline in ACSF. ACSF was composed of (in mM): 124 NaCl, 26 $NaHCO_3$, 2.5 KCl, 1 $CaCl_2$, 1.4 $MgCl_2$, 1 NaH_2PO_4, and 10 glucose, and was saturated with 95% O_2–5% CO_2, pH 7.4. In some experiments the extracellular recording solution was supplemented with 10 μM nifepidine (in 0.2% DMSO) to reduce Ca^{2+} currents. Blind and visually guided whole-cell patch recordings were obtained at 23°C from CA1 pyramidal neurons using thin-walled 2.8–5.5 MΩ glass pipettes filled with a solution composed of (in mM): 110 Cs-gluconate, 40 HEPES, 5 $MgCl_2$, 2 Na-ATP, 0.6 EGTA, and 0.3 Na-GTP, with the pH adjusted to 7.3 using CsOH; osmolality was 275–290 mOsm. In some experiments, EGTA was omitted, 40 mM HEPES was replaced with 5 mM HEPES plus 30 mM CsCl, and the solution was supplemented with 1 mM QX-314 (Sigma, St. Louis MO); similar results were obtained with both internal solutions. The presence of intracellular Cs^+ should block $GABA_B$ receptor-mediated currents. Brief (<100 msec) pulses of NMDA (0.3–2 mM) plus glycine (0.1–0.3 mM) were applied via pressurized pipette placed either in or just above stratum radiatum; the pressurized pipette was positioned to apply drug to the proximal third of the CA1 pyramidal cell dendrite; dilution at the tip was minimized before recording, and the tip was checked for blockage at the end of the experiment. NMDA-evoked currents were recorded at −70 mV (corrected for the +10 mV measured junction potential) before, during, and after thrombin application. In some experiments, membrane potential was changed to −40 mV during alternate agonist applications, or briefly jumped to −70 and −40 mV from a holding potential of 0 mV before and during agonist application. Series resistance (mean 23.4 ± 2.3 MΩ) was monitored from the instantaneous current response to a −5 mV jump applied before agonist application, and the membrane resistance (mean 1.4 ± 0.2 GΩ) was estimated from the leak current at −70 mV assuming a reversal potential of 0 mV. Series resistance compensation was not used because the mean response amplitude (−49 pA) will cause only a 1 mV error in the holding potential, and the slow response time course eliminates the capacitative component of series resistance filtering. Experiments with substantial changes in membrane or series resistance, regenerative currents, or development of leak currents exceeding −200 pA at −70 mV were excluded from analysis. After 3–10 stable baseline measurements were taken, 3 U/ml α-thrombin (Calbiochem, La Jolla CA; Sigma, St. Louis MO; Hematological Technologies, Essex Junction, VT) was applied through the bath solution for 10–18 min. In control experiments, ACSF was applied through the same perfusion line as thrombin. The perfusion line and recording chamber were washed extensively after experiments involving thrombin treatment because low picomole levels of α-thrombin are capable of inactivating PAR receptors before recording (Vu et al., 1991). The specific activity of the α-thrombin from various vendors ranged between 1720 and 3200 NIH U/mg by comparison to Lot J of the NIH standard. To estimate the concentration of active α-thrombin that corresponds to 1 U/ml activity, we calculated a conversion factor using our most pure α-thrombin (3200 U/mg). Because the protein in this lot was reported by the manufacturer to be >95% α-thrombin as determined by gel electrophoresis, a solution with 1 U/ml α-thrombin should be 9 nM using a molecular weight for thrombin of 36.7 kDa. For simplicity, we used a conversion factor of 1 U/ml = 10 nM α-thrombin throughout the text to estimate the concentration of active α-thrombin (hereafter referred to as thrombin) from various vendors. The peak potentiation of NMDA responses by thrombin was calculated over 20 min after thrombin application as the ratio of the highest running average of three consecutive response amplitudes (excluding the first 3 min after thrombin application) to the average of the three responses surrounding the time of thrombin application. Peak potentiation was used as a measure of the actions of thrombin to remove the variability associated with the time required for thrombin to reach cells at different depths in the slice.

Imaging of Fluo-3 fluorescence from cultured hippocampal neurons. Embryonic day (E)17–E19 rat pups were taken from CO_2-asphyxiated pregnant rats, and the hippocampus was dissected. Neurons were dissociated by trituration through a sterile fire-polished Pasteur pipette, centrifuged, and plated in Neurobasal (Life Technologies, Gaithersburg, MD) defined media at a density of 60,000/ml on polylysine-coated (10 μg/ml) 12 mm glass coverslips. Media was supplemented with B27 nutrients (Life Technologies) plus penicillin/streptomycin, and cells were maintained for 3–5 d at 37°C in humidified 5% CO_2. Neurons were incubated for 30–45 min in a solution composed of (in mM): 150 NaCl, 3 KCl, 10 HEPES, 2 $CaCl_2$, 20 mannitol, 10 glucose supplemented with 0.1% pluronic acid, 0.5% DMSO, and 3 μM Fluo-3 acetoxymethyl ester (Molecular Probes, Eugene OR); dye-loaded cells were placed in an identical solution lacking DMSO, pluronic acid, and Fluo-3. Images were acquired every 15 sec after 1 sec exposure to 450–490 nm light, and fluorescence was recorded through a bandpass filter (500–550 nm) using a Photometrics CC200 CCD camera; 3 nM thrombin (0.3 U/ml) ± 50 nM D-Phe-Pro-Arg-chloromethylketone (PPACK; an irreversible thrombin inhibitor) (Tapparelli et al., 1993) as well as 10 μM PAR agonist peptide SFLLRN were applied in the presence of 0.5 μM tetrodotoxin and 50 μM APV. NMDA (50 μM) and glycine (10 μM) were subsequently applied in the presence of 0.5 μM tetrodotoxin. Fluorescence intensity was measured in cell bodies using image analysis software (Scion Corporation, Frederick, MD) and expressed as F/F_o where F_o is the fluorescence intensity before drug treatment. Increases in fluorescence greater than 1.2-fold were considered to be real changes because untreated cells possessed a peak F/F_o ratio of 1.1 ± 0.04 over a typical experiment.

Transmitted light measurements in hippocampal slices. Rat hippocampal slices were prepared as described above and were bathed in a submerged chamber with 0.5 μM TTX and 3–7 U/ml thrombin in 0.5 μM TTX applied for 10–20 min. The intensity of transmitted light (450–490 nm) through hippocampal slices was monitored as an indication of extracellular volume fraction (Andrew and MacVicar, 1994). Images were recorded using a Princeton Micromax CCD camera (Trenton, NJ) (0.2 sec exposure every 20–40 sec) and analyzed using Axon Imaging Workbench 2.1 software (Foster City, CA). Intensity was expressed as I/I_o, where I_o is the intensity of transmitted light before treatment. Solutions were made hyperosmotic by addition of 30 mM mannitol, which can produce a 10% expansion of the extracellular volume fraction (McBain et al., 1990). Hypo-osmotic solutions were obtained by addition of 10% v/v water.

Genotyping of PAR1 −/− mice. Male PAR1 +/− mice were obtained from University of California San Francisco (gift from Dr. Shaun Coughlin) and have been described elsewhere (Connolly et al., 1996). PAR1 +/− (C57Bl/6 background) mice were bred with female C57Bl/6 wild-type mice from Jackson Laboratories (Bar Harbor, ME), and the presence of PAR1 or neomycin gene was determined using PCR of genomic tail DNA obtained by digesting tails in 0.7 ml of a solution containing 0.1 M EDTA, 50 mM Tris, 0.5% SDS, 1 mg/ml proteinase K, pH 8.7, at 50–55°C for 4–5 hr; the digest was subsequently extracted with phenol/chloroform. The DNA was precipitated and resuspended at 1 μg/μl in Tris/EDTA (10 mM/1 mM). PCR reactions were run with 1 μg genomic DNA using the following protocols repeated through 40–45 cycles: 95°C (30 sec), 85°C (5 sec), 60°C (2 min), 72°C (2 min) for PAR1 +/+ mice, and 95°C (30 sec), 85°C (5 sec), 58.5°C (45 sec), 72°C (1 min) for the neomycin resistance gene. The primers for PAR1 have been described (Connolly et al., 1996); for neomycin the primer pair GAAGGGACTTGCTATTGG, GCTCTTCAGCAATATCACGGG was used, which generates a 431 bp fragment. PCR reactions testing the genotype of unknown animals were performed in parallel with control DNA from PAR1 +/+, PAR1 +/−, and PAR1 −/− mice. Mice used in this study were derived from PAR1 −/− breeding pairs (11), PAR1 +/+ breeding pairs (4), or Jackson Laboratories wild-type mice (11). PCR results were repeated three times for all mice included in the study.

Expression and recording of NMDA and PAR1 receptor function in Xenopus laevis *oocytes.* cRNA was synthesized from linearized template

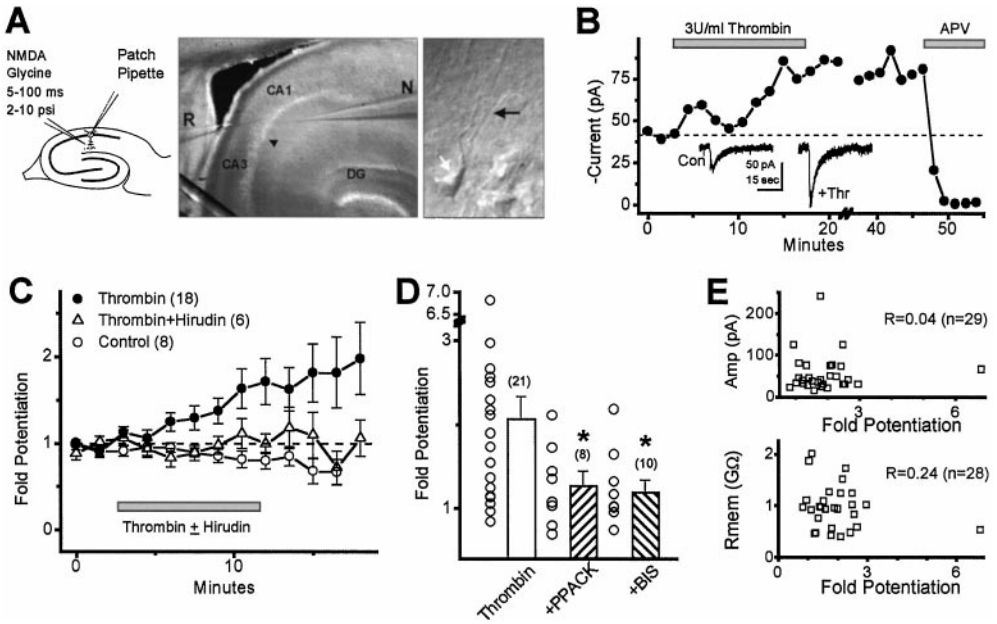

Figure 1. *A*, The diagram illustrates our experimental arrangement. The photomicrographs show typical placement of the pressurized pipette (*N*) in relation to recording pipette (*R*) in stratum pyramidale. The typical placement of the NMDA containing pipette (*black arrow*) is shown in relation to a single CA1 pyramidal cell (*white arrow*). The *black arrowhead* shows the CA1/CA3 boundary. *B*, Time course of current–response amplitude to NMDA during 3 U/ml thrombin application. *Inset*, Representative current–responses from this same cell to pressure-ejected 1 mM NMDA and 100 μM glycine were recorded at −70 mV before and during perfusion with 3 U/ml thrombin (30 nM). APV (100 μM) blocked the response to NMDA/glycine. *C*, Mean time course (±SEM) of current responses to NMDA plus glycine in cells treated with 3 U/ml thrombin or 3 U/ml thrombin + 100 ATU hirudin. The number of cells is indicated in *parentheses*. The mean response time course is also shown for control cells that were superfused with ACSF. *D*, Mean potentiation (±SEM) of NMDA receptor responses by thrombin (*open bar*; −70 mV) was blocked by an irreversible serine protease inhibitor with high selectivity for thrombin over plasmin. PPACK (500 nM) (~15× thrombin concentration) was preincubated for 5–15 min with 30 nM thrombin before application to slices. Some slices were pretreated with 10 μM bisindolylmaleimide (*BIS*) for 10 min. $^*p < 0.05$ compared with thrombin potentiation; Kruskal–Wallis ANOVA, Dunn *post hoc* test. *Open circles* show results from individual neurons. *E*, Scatter plot of the NMDA response amplitude (*top panel*) versus fold-potentiation by thrombin and membrane resistance versus fold-potentiation by thrombin (*bottom panel*). There was no significant correlation between these parameters or the level of thrombin-induced potentiation ($p < 0.5$). Data from rat and mouse were pooled.

cDNA according to manufacturer specifications (Ambion, Austin, TX). *Xenopus* oocytes were removed from ovaries of female frogs anesthetized with 0.3% 3-aminobenzoic acid ethylester. Groups of 20–30 stage V–VI oocytes were incubated in 292 U/ml Worthington (Freehold, NJ) Type IV collagenase for 2 hr with slow shaking. The oocytes were rinsed in Barth's solution and stored at 17°C in Barth's solution supplemented with 100 μg/ml gentamycin and 40 μg/ml streptomycin. Control oocytes were injected with 3 ng NR1 subunit and 7 ng NR2B subunit. Other oocytes were injected with the NMDA receptor subunits plus 3 ng PAR1 cRNA. Two-electrode voltage-clamp recordings were made 3–7 d after injection. Oocytes were continually perfused with recording solution (90 mM NaCl, 1 mM KCl, 10 mM HEPES, pH 7.4) and held under voltage clamp at −30 to −50 mV with an OC-725B amplifier (Warner Instruments, Hamden, CT). Recording solution was supplemented with 1.0 mM $CaCl_2$ during initial impalement of the oocytes and subsequently 0.5 mM $BaCl_2$ during recording to reduce the calcium-activated chloride current endogenous to oocytes. Voltage and current electrodes had a resistance of 3–6 MΩ when filled with 0.3–3 M KCl. NMDA receptor currents were evoked by 20 μM glutamate/10 μM glycine perfused for 0.5–1 min. PAR1 receptor activation was elicited by either 2.5 U/ml thrombin (Calbiochem) or 10–30 μM agonist peptide SFLLRN (Bachem, Torrance, CA) for 2–3 min; the recording chamber and perfusion lines were washed extensively between thrombin applications because low picomole levels of thrombin are capable of inactivating PAR receptors before recording (Vu et al., 1991). Expression of PAR1 protein was verified by a thrombin- or SFLLRN-stimulated rapidly desensitizing inward current at −30 mV that reflects the Ca^{2+}-activated Cl^- current endogenous to the oocyte (Miledi, 1982). To test the ability of thrombin to modify NMDA receptor function in oocytes, recordings of receptor function were made both before and after a 15–60 min incubation in recording solution supplemented with thrombin in Eppendorf tubes at room temperature. Only oocytes that showed <10% change in current between a pair of responses within each 10 min recording period were included in the analysis, to eliminate possible rundown of response. Oocytes with responses <50 nA were not included in the analysis.

NMDA receptor subunit immunoblots. Human embryonic kidney (HEK) cells were maintained in DMEM supplemented with 0.5 mM glutamine, 1 mM pyruvate, penicillin, streptomycin, and 10% fetal bovine serum in a humidified environment with 5% CO_2, and transfected with 1 μg/ml NR1 or 1:2 μg/ml NR1/NR2 cDNA (Chen and Okayama, 1987). Cells were washed in ice-cold HEPES-buffered saline (HBS) and scraped on ice, and membranes were isolated by centrifugation at 12,000 × *g*. N-terminal *myc*-tagged NR1–1a was a gift from Dr. R. Huganir (Johns Hopkins University, Baltimore, MD) and was constructed by inserting a *myc* tag (MEQKLISEEDLN) after Asn50, 29 residues after the signal peptide. Adult rat brain regions were dissected, frozen in liquid nitrogen, homogenized in ice-cold HBS, centrifuged, and stored at −20°C. Membranes were resuspended in HBS and treated with thrombin or buffer for 30 min at 37°C. Samples were centrifuged, and the membrane pellet was resuspended in 2% SDS, 62.5 mM Tris, 10% glycerol, 5% β-mercaptoethanol, 0.05% bromophenol blue, pH 6.8; some samples were treated with 10 U DNase for 10 min at 37°C. SDS-PAGE and protein blotting to Immobilon-P membranes were performed as described (Lau and Huganir, 1995). Membranes were blocked for 30 min in 0.2 M Tris base, 1.37 M NaCl, pH 7.4, containing 5% nonfat dry milk, and incubated overnight at 4°C in primary antibodies: NR1 mAb54.1 (gift from Dr. S. Heinemann, Salk Institute, La Jolla, CA), NR1 alt-C-terminal (Upstate Biotechnology, Lake Placid, NY), NR2A C-terminal (Chemicon, Temecula, CA), or NR2B C-terminal (Upstate Biotechnology). Membranes were washed three times and incubated with HRP-conjugated goat anti-mouse or goat anti-rabbit antibodies (1:10,000), washed three times, and developed using enhanced chemiluminescence. The percentage of receptor cleaved by thrombin was determined using densitometry.

RESULTS

Thrombin potentiation of NMDA receptor currents in rat hippocampal neurons

Messenger RNA encoding the thrombin receptor PAR1, which is known to activate G_O- and G_I-linked intracellular signaling systems (Grand et al., 1996; Dery et al., 1998), is expressed in hippocampal neurons including CA1 pyramidal cells (Weinstein et al., 1995; Niclou et al., 1998). We have studied the effects of thrombin on whole-cell voltage-clamp recordings of rat CA1 hippocampal pyramidal neuron responses to pressure application of NMDA plus glycine into the dendritic field to test whether serine proteases can alter NMDA receptor function through PAR1 activation. Figure 1*A* illustrates our experimental record-

ing arrangement. NMDA receptor current responses were evoked in the presence of 1 μM tetrodotoxin and 10 μM bicuculline. Typical NMDA-evoked current responses recorded at −70 mV are shown as a time course before and during the application of 30 nM thrombin (3 U/ml) for a representative cell (Fig. 1*B*). In this cell, thrombin treatment potentiated the current response with a time course consistent with thrombin diffusion into the tissue. To confirm that the enhanced inward current response arises from activation of NMDA receptors rather than strychnine-sensitive glycine receptors or sensitization of stretch-activated channels that might respond to pressure ejection of agonist, responses to NMDA–glycine were blocked by 100 μM of the competitive NMDA receptor antagonist APV ($n = 7$ cells). Thrombin potentiation of NMDA responses in neurons with the pressurized pipette positioned <100 μm above the slice ruled out the possibility that thrombin sensitized the tissue to pressure. Thrombin produced on average a 2.07 ± 0.27-fold peak potentiation (mean ± SEM; $n = 21$) of NMDA responses at −70 mV within 20 min compared with cells in which thrombin was not applied (Fig. 1*C*). Although potentiation was often rapid (within a few minutes) (Fig. 1*B*,*C*), in some cells thrombin potentiation continued to increase with time, reaching peak levels between five- and eightfold. The thrombin-induced peak potentiation of NMDA responses appeared to possess a bimodal distribution in which a subset of the cells showed little response to thrombin (Fig. 1*D*). This differential effect of thrombin is consistent with the expression of PAR1 mRNA observed in some but not all CA1 pyramidal cells (Weinstein et al., 1995; Niclou et al., 1998).

On average there were no significant changes in series resistance (111 ± 7%; $p < 0.2$; paired *t* test) during thrombin application. Average membrane resistance (1.2 ± 0.1 MΩ) decreased modestly throughout the course of the experiment; however, this decrease was not significantly different between thrombin-treated (12 ± 6%) and control slices (16 ± 7%; $p < 0.2$; *t* test). In addition, there was no significant correlation ($p < 0.5$ in all cases) between the levels of thrombin potentiation and the following parameters: the series resistance ($r = 0.37$), the change in series resistance ($r = 0.00$), the membrane resistance ($r = 0.24$) (Fig. 1*E*), the change in membrane resistance ($r = 0.18$), or the response amplitude ($r = 0.04$) (Fig. 1*E*). Current responses recorded under voltage clamp to pressure application of NMDA reversed sign at +0.1 mV ($n = 6$). Together these results suggest that the thrombin-induced potentiation of NMDA receptor function that we observed does not reflect a thrombin-induced compromise of the voltage clamp. Indeed, an identical degree of thrombin potentiation of the NMDA response (1.8 ± 0.2-fold) was observed in cells not included in Figure 1*D* because either their input resistance was too low or there was an increase in series resistance throughout the experiment ($n = 12$). Furthermore, thrombin-induced potentiation was observed when cells were held at 0 mV to inactivate Ca^{2+} channels, and the holding potential briefly stepped to −70 mV before and during agonist application (2.7 ± 0.7-fold potentiation; $n = 7$). There was no significant difference between the degree of potentiation seen under normal conditions or in cells held at 0 mV ($p > 0.05$; Mann–Whitney test). These results argue against the possibility that asynchronous activation of PAR1/PKC-potentiated (e.g., Hall et al., 1995) Ca^{2+} channels during NMDA-induced loss of voltage clamp in distal dendrites could account for the potentiation that we observed.

To confirm that the potentiating effects of thrombin that we observed reflect the proteolytic actions of thrombin rather than nonspecific effects or the actions of other contaminant proteases, we evaluated whether the potentiation of NMDA receptor responses by thrombin could be blocked by two selective thrombin antagonists. We first examined whether hirudin (Calbiochem), an inhibitor that binds with high affinity to the anion binding exosite (K_D 20 fM) of thrombin, could alter the time course of thrombin potentiation of NMDA receptor function. Hirudin significantly reduced the potentiation by thrombin of NMDA responses (0.96 ± 0.23-fold; $n = 5$) (Fig. 1*C*) ($p < 0.05$; Mann–Whitney test for average potentiation 12–19 min after treatment). In a separate experiment, we premixed thrombin with an irreversible inhibitor of thrombin that covalently modifies the fibrinopeptide catalytic site for cleavage of substrate (500 nM PPACK) (Tapparelli et al., 1993) before application to the slice. The average peak potentiation of the NMDA response after thrombin–PPACK application was also significantly reduced (1.28 ± 0.17; $n = 8$) compared with thrombin treatment (2.07 ± 0.27-fold; $n = 21$) (Fig. 1*D*) (Kruskal–Wallis ANOVA, Dunn *post hoc* test; $p < 0.05$). Nonparametric statistical tests were used because of the non-normal distribution of peak fold potentiation by thrombin (Fig. 1*D*). These experiments confirm that the potentiation of NMDA receptor currents that we observed are caused by the proteolytic actions of thrombin on either a protease receptor such as PAR1 or some other substrate.

Because PAR1 is expressed in the CA1 region and is known to couple to the G_Q family of Gα-proteins, which can stimulate phosphoinositide hydrolysis, increase intracellular Ca^{2+}, and activate intracellular protein kinases (Grand et al., 1996), we tested whether the serine/threonine protein kinase inhibitor bisindolylmaleimide (BIS) could occlude thrombin potentiation of NMDA receptor function. When BIS (10 μM) was included in ACSF, potentiation of NMDA receptor currents by application of 30 nM (3 U/ml) thrombin was reduced to 1.20 ± 0.13-fold ($n = 10$, $p < 0.05$; ANOVA) (Fig. 1*D*), indicating that the potentiating effect of thrombin requires at least one functional protein kinase. NMDA responses were unchanged during preapplication of BIS, suggesting that BIS does not induce an inhibition of the NMDA response that is additive to potentiation.

Thrombin does not alter extracellular volume fraction in hippocampal slices

In vivo injection of thrombin into the brain can cause edema and tissue swelling (Lee et al., 1996), raising the possibility that the potentiation we observed of NMDA receptor responses to agonist applied from a point source might reflect a change in the spatial diffusion profile of NMDA and glycine secondary to thrombin-induced changes in extracellular volume fraction. For example, any changes in the extracellular volume fraction that amplified the concentration of pressure-ejected NMDA in the narrow clefts or expanded the tissue volume reached by NMDA would potentiate the NMDA response. To ensure that the diffusional characteristics of pressure-applied NMDA are not influenced by thrombin treatment, we measured the effects of thrombin application on transmitted light, which has previously been shown to be a sensitive measure of extracellular volume fraction (Andrew and MacVicar, 1994). Hippocampal slices (300 μm) were prepared and incubated in 0.5 μM TTX to abolish synaptic activity. Perfusion of these slices with solutions made hyperosmotic by addition of 30 mM mannitol reduced the transmitted light by 10% in both CA1 stratum radiatum and stratum pyramidale, consistent with expansion of the extracellular space (McBain et al., 1990; Andrew and MacVicar, 1994). Conversely,

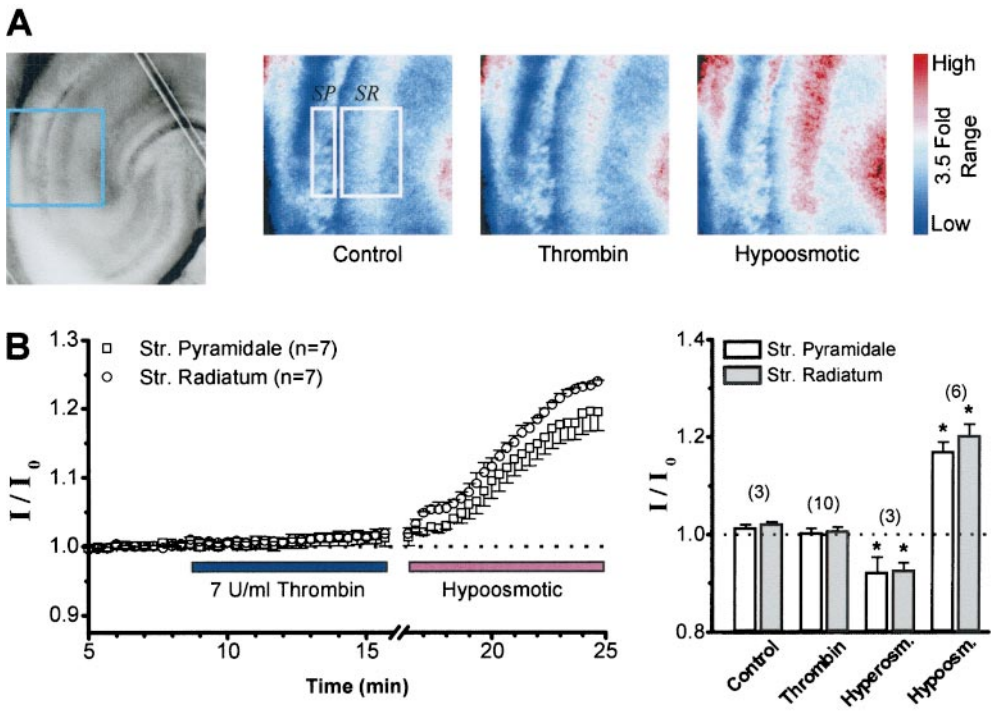

Figure 2. *A*, *Left panel*, Photograph of a 300 μm rat hippocampal slice with the region indicated in *blue* expanded to the *right*. *Right panels*, Pseudocolor representation of the relative intensity of transmitted light (500–550 nm) in a slice bathed in ACSF after treatment with 0.5 μM TTX (*Control*), 0.5 μM TTX plus 7 U/ml thrombin, or 0.5 μM TTX with ACSF made hypo-osmotic by addition of 10% v/v water. *Boxes* show regions from which average intensity measurements were made in this slice. *SP*, Stratum pyramidale; *SR*, stratum radiatum. The *color code* on the *right* indicates a 3.5-fold relative range of intensity. *B*, *Left panel*, Mean time course (±SEM) of the effects of thrombin or hypo-osmotic treatment on transmitted light in seven cells. Increased transmittance is correlated with reduced extracellular volume fraction (see Results) (Andrew and MacVicar, 1994). *Right panel*, Summary of experiments showing no effect of thrombin on mean relative transmitted light compared with hypo-osmotic ACSF or ACSF made hyperosmotic by addition of 30 mM mannitol. *Bars* show the mean ratio of transmittance after treatment (I) to control transmittance (I_0). * indicates significantly different from control measurements ($p < 0.05$; t test). The number of slices is indicated in *parentheses*.

hypo-osmotic solutions produced a 20% increase in transmitted light (Fig. 2*A*), consistent with induction of cell swelling. Treatment of slices with 3–7 U/ml of thrombin for 10–20 min produced no significant change in the intensity of transmitted light (I) in either stratum pyramidale ($I/I_o = 1.00 \pm 0.01$) or stratum radiatum ($I/I_o = 1.01 \pm 0.01$) compared with untreated slices (Fig. 2*B*). These data suggest that neither thrombin activation of PAR1 nor cleavage of other substrates significantly alters extracellular volume fraction in acute slices. We interpret these data to suggest that the potentiation of NMDA receptor responses that we observe after activation of PAR1 does not reflect a thrombin-induced change in the temporal–spatial diffusion profile of NMDA–glycine released into or above the tissue from our pressurized pipette.

Thrombin proteolysis of the NR1 subunit

Because one defining feature of thrombin is its proteolytic action, we examined whether NMDA receptor protein subunits were substrates for thrombin cleavage. Incubation of brain membranes with thrombin for 1 hr at 37°C resulted in the appearance of a new band that was 12 kDa ($n = 10$) lower in molecular weight than the parent band in immunoblots probed with an antibody to NR1 that recognizes the M3 M4 loop (mAb54.1; epitope between residues 660–811) (Siegel et al., 1994) (Fig. 3*A*). However, similar treatment of membranes did not induce any observable molecular weight shift of either the NR2A ($n = 8$) (Fig. 3*B*) or NR2B subunits ($n = 10$; 3–300 U/ml; data not shown). NR1 subunits in all brain regions tested were cleaved by high concentrations of thrombin (1–3 μM; 100–300 U/ml; $n = 5$–7 for each region). The degree of cleavage by both high and low concentrations of thrombin varied across regions, as shown in Figure 3*A*. Although cerebellar ($n = 7$), cortical ($n = 5$), and brainstem ($n = 5$) NR1 subunits were insensitive to cleavage by 300 nM thrombin (30 U/ml), 30 nM thrombin (3 U/ml) cleaved 20% of the NR1 subunit in hippocampal membranes ($n = 7$) and 50% of NR1 in striatal membranes ($n = 10$), suggesting that receptors in these membranes are more sensitive to the effects of thrombin. In addition, 1–3 μM thrombin cleaved 100% or subunits in all brain regions (Fig. 3*C*) except striatum, where the maximal observed cleavage of 52% suggests that a thrombin-resistant population of NR1 subunits exists. Thrombin-induced NR1 cleavage does not involve PAR1 receptor-activated second messenger systems because 0.1–1 mM PAR1 peptide agonist SFLLRN did not stimulate cleavage ($n = 3$) (Fig. 3*C*). In addition, 100 ATU hirudin, a thrombin inhibitor, blocked cleavage of NR1 in striatal membranes by 30 nM thrombin ($n = 3$), suggesting that the shift in the molecular weight of the NR1 subunit does not reflect the actions of contaminant proteases.

Recombinant NR1 subunits transiently expressed in HEK 293 cells were also sensitive to thrombin cleavage. Thrombin (10–1000 U/ml) cleaved both homomeric NR1–1b receptors ($n = 9/10$ experiments) and heteromeric NR1–1b/NR2B receptors ($n = 6/6$ experiments; data not shown). The appearance of a new NR1 band of reduced molecular weight in thrombin-treated brain membranes was detected using mAb54.1, which recognizes an epitope located near the M3 transmembrane region (Fig. 3*F*) (Siegel et al., 1994). To evaluate the location of the thrombin cleavage site, we assessed the effects of thrombin on a recombinant NR1–1a subunit that contained a *myc* epitope inserted into the N terminal after Asn50. Thrombin induced a similar shift in molecular weight for N-terminal *myc*-tagged NR1 as observed for the recombinant and native receptors detected with mAb54.1 (Fig. 3*D*) ($n = 3$), suggesting that cleavage likely occurs near the C terminal of the receptor. Consistent with this idea, deletion of the C-terminal portion of NR1–1b by replacement of the coding sequence starting at amino acid position 785 with a cDNA encoding HLEGPIL-stop abolished any detectable cleavage of the NR1 subunit (Fig. 3*E*) ($n = 3$). These data suggest that thrombin cleaves NR1 subunit somewhere near the C terminal (Fig. 3*F*)

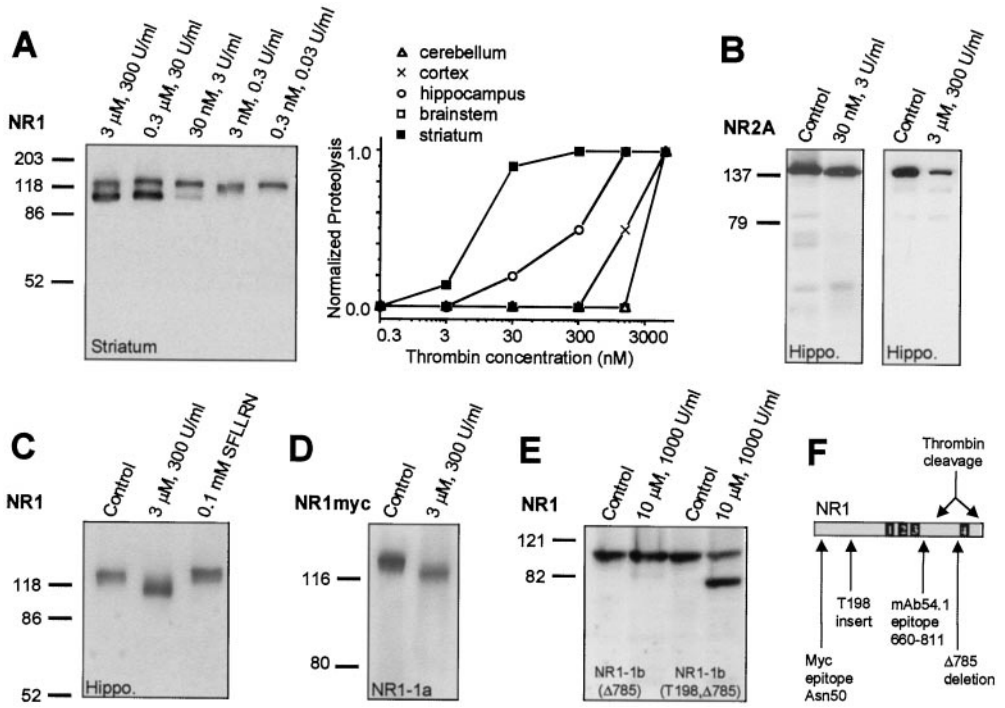

Figure 3. A, *Left panel*, Immunoblot analysis showing thrombin cleavage of striatal NR1 subunit in membrane homogenates detected with mAb54.1. *Right panel*, The concentration dependence of thrombin cleavage of the NR1 subunit is shown for various brain regions. The degree of cleavage has been normalized to 1.0 to facilitate comparison of the thrombin sensitivity. One hundred percent of NR1 was cleaved in all brain regions except striatum, which showed maximum 52% cleavage. Measurements are the mean of five experiments. *B*, Immunoblot analysis showing the thrombin insensitivity of hippocampal NR2A detected with a C-terminal antibody. No new bands were observed after the treatment of NR2A with low or high concentrations of thrombin. *C*, Thrombin treatment of hippocampal NMDA receptors reduces the molecular weight of NR1, detected with mAb54.1. Treatment of membranes with a supramaximal concentration of the PAR1 peptide agonist SFLLRN did not alter the molecular weight of NR1. *D*, Thrombin treatment of recombinant NR1–1a subunits engineered to include a sequence encoding a *myc* tag at the N terminal and expressed in HEK cells (see Materials and Methods) detected with a *myc* antibody caused a similar molecular weight shift as for thrombin-treated neuronal receptors. *E*, Thrombin treatment did not alter the molecular weight of recombinant NR1–1b subunits with the C terminal deleted after residue 785 (NR1Δ785). Thrombin treatment of the same deletion construct engineered to express a thrombin cleavage site (LVPRGS) starting at residue 198 in exon 5 verified that thrombin was active in the experiment because a band corresponding to the predicted molecular weight for cleavage at exon 5 was observed. *F*, Linear map of the NR1 gene product showing the relative positions of the engineered *myc* and mAb54.1 epitopes, the engineered thrombin cleavage site, the Δ785 deletion, and the region predicted from these results to harbor the thrombin cleavage site. *Black boxes* are membrane-associated domains.

and were consistent with immunoblots performed using a C-terminal antibody (Fig. 4*B*). However, use of a C-terminal antibody recognized a larger cleavage product than predicted from data in Figure 3. The reasons for the discrepancy in the molecular weight of the C-terminal NR1 cleavage product from brain membranes as detected with different antibodies are under investigation.

To test whether the potentiation of NMDA responses that we observed in hippocampal neurons treated with low concentrations of thrombin for short periods of time (12–20 min at 23°C) was related to proteolysis of the NR1 subunit, the CA1 region was microdissected after electrophysiological experiments and analyzed by SDS-PAGE followed by immunoblot. The results of one such experiment are shown in Figure 4. Despite robust potentiation of the NMDA receptor response during the 15 min of 3 U/ml thrombin application (Fig. 4*A*), no NR1 cleavage product was observed in immunoblots of membranes obtained from the CA1 region microdissected immediately after the experiment (Fig. 4*B*). Similar results were obtained from six slices, which are consistent with data in Figure 3*A* that show only modest (~20%) cleavage of hippocampal NR1 subunit by four times longer thrombin treatments (1 hr incubation at 37°C with 3 U/ml thrombin). If cleavage of NR1 by 3 U/ml thrombin is linearly related to time and temperature sensitive with a Q_{10} of 2.5, we predict from the 20% cleavage of hippocampal NR1 after 1 hr at 37°C that thrombin should cleave 1% of the NR1 protein after 15 min treatment of our slices at 23°C, which is likely below our limit of detection. In addition, there was no significant difference in the response amplitude of recombinant NR1/NR2A and NR1/NR2B NMDA receptors expressed in *Xenopus* oocytes, which lack thrombin receptors (Vu et al., 1991) that were treated either with buffer or identical thrombin concentrations and incubation conditions used in slice experiments (3 U/ml; 15 min; 23°C) (Fig. 4*C*). Incubation of oocytes with higher concentrations of thrombin (300–1000 nM) for 60 min reduced current–response amplitude to 42 ± 9% ($n = 7$), compared with 78 ± 5% ($n = 6$; $p < 0.05$, t test) for buffer-treated controls, suggesting that thrombin can inhibit NMDA receptor function, presumably through cleavage of NR1. These and other results (see below) suggest that the thrombin-mediated potentiation of the NMDA current responses in CA1 hippocampal pyramidal neurons does not reflect NR1 proteolysis or direct interaction of thrombin with NMDA receptors.

Thrombin potentiation of NMDA receptor function is PAR1 dependent

To evaluate the working hypothesis that thrombin activation of the protease receptor PAR1 leads to potentiation of NMDA receptor secondary to activation of intracellular signaling pathways, we first verified that hippocampal neurons contain functional protease receptors, which are known to couple to the G_Q family of Gα-proteins (Yang, 1997). We measured increases in fluorescence of the calcium-sensitive dye Fluo-3 in response to 3 nM thrombin or 10 μM PAR1 peptide agonist SFLLRN. This peptide matches the new N terminal of PAR1 that is revealed by thrombin cleavage at Arg41 and is thought to act as a tethered activator of the receptor (Fig. 5*A*,*B*). Experiments were performed on cultured neurons in the presence of 0.5 μM TTX to reduce the synaptic activity and 50 μM APV to eliminate the possibility that thrombin potentiation of tonically active NMDA

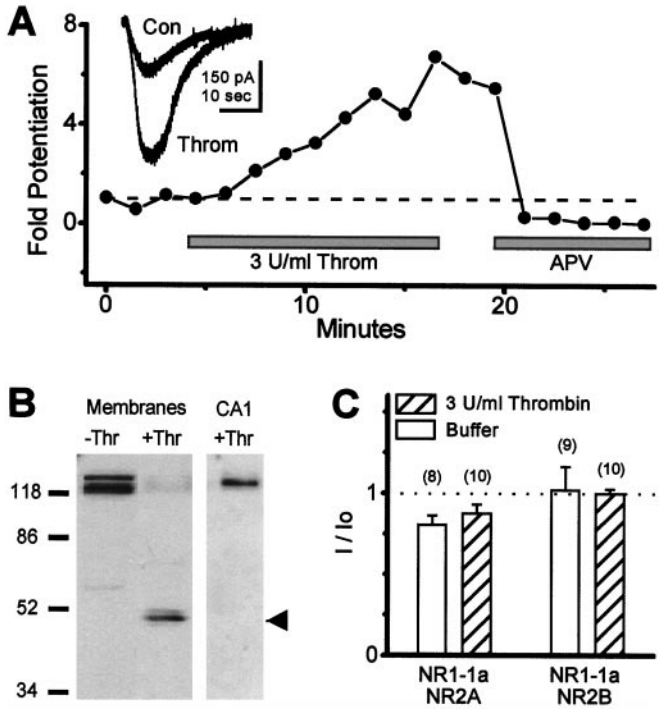

Figure 4. *A*, The time course of the response amplitude for a CA1 pyramidal cell that exhibits robust potentiation during thrombin treatment is shown. *Inset*, Current–responses before and after thrombin (3 U/ml) treatment of the slice are superimposed. Application of 100 μM APV completely inhibited the response. *B*, Immunoblot analysis using a C-terminal NR1 antibody of microdissected CA1 region after thrombin treatment from the slice shown in *A* confirms that our thrombin treatment did not cause proteolytic cleavage of the NR1 subunit. The control lane shows the position of the expected cleavage band in brain membranes treated with 300 U/ml thrombin. *C*, Treatment of NR1/NR2A and NR1/NR2B recombinant receptors expressed in *Xenopus* oocytes with the same concentration of thrombin (3 U/ml) and the same duration (15 min) used in slice experiments did not significantly alter the mean response amplitude (±SEM) compared with buffer-treated oocytes (*t* test). The mean fold potentiation by thrombin is shown and was calculated from each oocyte as the ratio of the post-treatment current (I) to the pretreatment current (I_0).

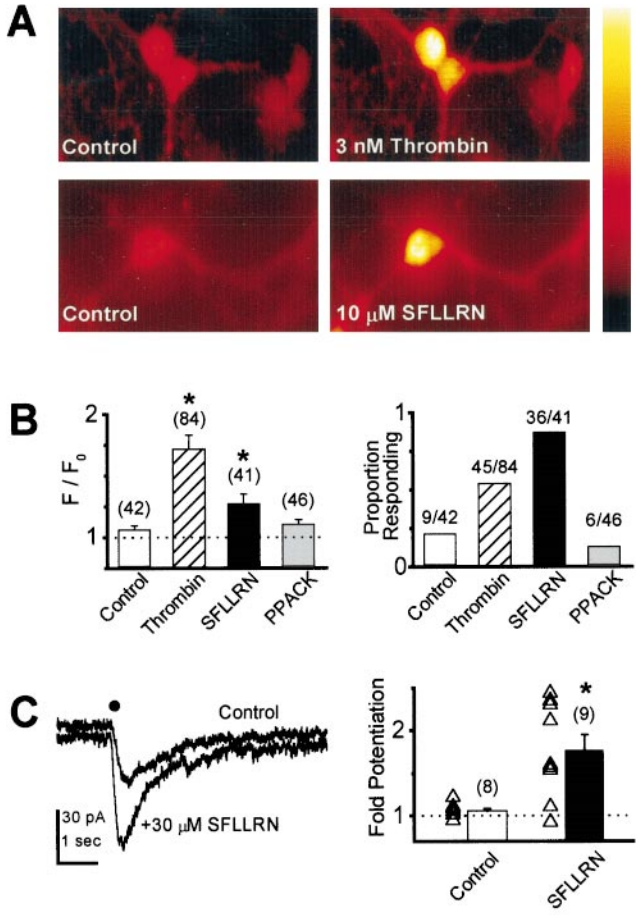

Figure 5. *A*, Thrombin and PAR1 peptide agonist SFLLRN increase somatic Fluo-3 fluorescence in cultured hippocampal neurons. The peak fluorescence increase in the experiments shown was 3.45- and 2.23-fold for SFLLRN and thrombin, respectively. The *bar* on the *right* shows pseudocolor scale representation of fluorescence intensity (*black* = lowest intensity, *yellow* = highest intensity). *B*, *Bar graphs* summarize the results from Fluo-3 imaging experiments, which demonstrate the expression of thrombin- or peptide agonist-responsive receptors in some cultured neurons. *Left panel* shows mean (±SEM) peak Fluo-3 fluorescence as fold increase (F/F_o) induced by 0.3 U/ml (3 nM) thrombin, 10 μM peptide agonist SFLLRN, or 3 nM thrombin preincubated with 50 nM of the thrombin inhibitor PPACK. * indicates significantly greater than control ($p < 0.05$; *t* test). Fluo-3 fluorescence increased in response to thrombin or SFLLRN within a few seconds and relaxed toward baseline over the next 10 min. *Right panel* summarizes number of neurons that responded to PAR1 activation; only cells that responded to NMDA with an increase in Fluo-3 fluorescence were considered to be neurons and included in the analysis. *C*, *Left panel* CA1 pyramidal cell current–responses to pressure-applied NMDA/glycine before and during SFLLRN application; *circle* shows time of NMDA/glycine application. *Right panel*, Mean peak fold potentiation (±SEM) of the NMDA receptor responses in rat CA1 pyramidal cells by 30 μM (~10× EC_{50}) (Gerszten et al., 1994) of the PAR peptide agonist SFLLRN is compared with cells treated with ACSF. Holding potential was −70 mV. Number of cells is indicated in *parentheses*. *$p < 0.05$; Mann–Whitney test.

receptors (Sah et al., 1989) might increase intracellular Ca^{2+}. Images were acquired while the following sequence of solutions was perfused into the chamber: TTX/APV, TTX/APV/thrombin or SFLLRN, TTX/APV, TTX/NMDA/glycine. Both thrombin and the PAR1 peptide agonist SFLLRN elicited a robust increase in the Fluo-3 fluorescence in both the soma and dendrites of a subset of neurons, suggesting that these treatments increased intracellular Ca^{2+}. The thrombin inhibitor PPACK (50 nM) reduced the percentage of neurons responding to thrombin and the response magnitude to control levels (1.1 ± 0.04-fold; $n = 46$) (Fig. 5*B*). Because we could detect no proteolysis of NR1 in the slices that we studied, the most likely explanation for the potentiation that we observed after thrombin treatment was that thrombin activated PAR receptors on CA1 pyramidal cells. To directly evaluate this possibility, we tested whether the specific PAR1 agonist peptide SFLLRN, which mimics the new N terminal on PAR1 revealed after thrombin cleavage after Arg41, could also potentiate NMDA receptor responses in CA1 pyramidal cells in acute hippocampal slices. Figure 5*C* summarizes the results of this experiment and shows that application of 30 μM PAR agonist SFLLRN (10× EC_{50}) to the slice produced a 1.76 ± 0.19-fold ($n = 9$) potentiation of the response to pressure-applied NMDA plus glycine, which was significantly different from that observed in buffer-treated slices (1.05 ± 0.03-fold potentiation; $n = 8$; $p < 0.01$ Mann–Whitney test). These data are consistent with the idea that thrombin potentiates NMDA receptors through activation of a protease receptor, most likely PAR1.

To further evaluate the role of PAR1 activation in thrombin-induced potentiation of NMDA receptor responses, we studied

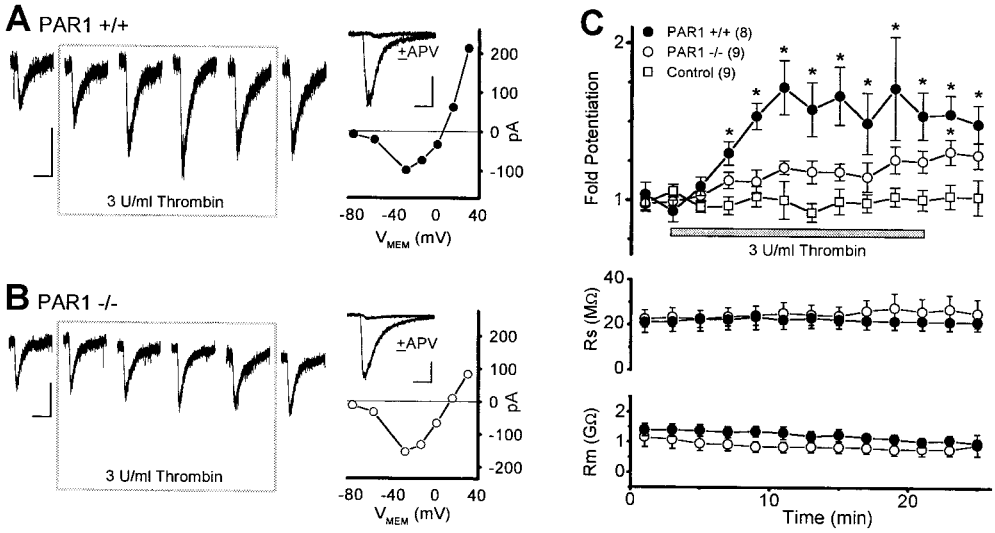

Figure 6. *A*, *B*, *Left panels*, Raw current traces from every fourth NMDA application recorded at −70 mV (i.e., every 4 min) are shown for CA1 pyramidal cells from PAR1 +/+ C57Bl/6 mice (*A*) and PAR1 −/− C57Bl/6 mice (*B*). *Gray boxes* show periods of thrombin application. Calibration, 10 sec, 20 pA. *Right panels*, APV (100 μM) blocked NMDA responses recorded at −40 mV (calibration, 5 sec, 50 pA); NMDA responses reversed near 0 mV. *C*, Mean time courses (±SEM) of thrombin (3 U/ml)-induced potentiation of NMDA responses in CA1 pyramidal cells from PAR +/+ and PAR1 −/− C57Bl/6 mice were compared with that of mice (PAR1 +/+, −/−) treated with ACSF. * indicates significantly different from ACSF-treated slices ($p < 0.05$; Kruskal–Wallis test; Dunn *post hoc* test). There were minimal changes in the series resistance or membrane resistance during the course of the experiment (*bottom panels*).

the effects of thrombin application on hippocampal CA1 pyramidal cells from wild-type mice as well as mice engineered to lack the full-length PAR1 gene (Connolly et al., 1996). Application of 3 U/ml of thrombin caused a robust potentiation of responses to pressure-applied NMDA plus glycine in wild-type C57Bl/6 mice that was significantly different at all times from that observed in control experiments in which ACSF was applied (Fig. 6). However, application of thrombin to PAR1 −/− C57Bl/6 mice did not significantly increase NMDA receptor responses. Series and membrane resistance were monitored throughout the experiment and showed only modest changes that could not account for the different effects of thrombin. As in rat hippocampal slices, NMDA receptor response in wild-type and PAR1 −/− mice were abolished by 100 μM APV ($n = 9$) after thrombin treatment, suggesting that any potentiation observed reflected NMDA receptor activation rather than sensitization of the cells to glycine or pressure. Although these experiments provide direct evidence for the involvement of PAR1 in thrombin-induced potentiation of NMDA receptor function, modest levels of thrombin potentiation of NMDA receptor responses still develop slowly in PAR1 −/− mice, becoming significant only after thrombin application. This latent potentiation in PAR1 −/− mice raises the possibility that thrombin cleavage of as yet uncharacterized PARs or other signaling substrates in hippocampal neurons might lead to modest levels of NMDA receptor potentiation observed in PAR1 −/− mice.

Potentiation of recombinant NMDA receptors by activation of the thrombin receptor PAR1

To test whether PAR1 activation can directly alter NMDA receptor function in recombinant systems, we injected *Xenopus* oocytes with cRNA encoding NMDA receptor subunits alone or together with cRNA encoding the PAR1 receptor. The oocytes were placed under two-electrode voltage clamp to record agonist-evoked currents at a membrane holding potential of −30 mV in Mg^{2+}-free solutions (Fig. 7). Recordings were made in a paired fashion such that two oocytes, one of which was coinjected with PAR1, were recorded from simultaneously with the same solutions. The presence of functional PAR1 receptor was confirmed by observation of the Ca^{2+}-activated Cl^- current during a 2–3 min application of 0.03–3 U/ml (300 pM–30 nM) of thrombin. This inward current is observed when Ca^{2+} is released from intracellular stores after PAR1 activation of phosphoinositol-linked signaling (Miledi, 1982; Miledi and Parker, 1984; Vu et al., 1991). NMDA receptor responses in oocytes that were not coinjected with PAR1 cRNA ($n = 19$) were not potentiated by thrombin application, whereas oocytes that were injected with PAR1 cRNA typically displayed thrombin-induced potentiation of the NMDA receptor-mediated current ($n = 23$) (Fig. 7*A*,*B*). Potentiation of NR1–1a/NR2A receptors coexpressed with PAR1 was observed after treatment with 300 pM (1.37 ± 0.08-fold; $n = 7$), 3 nM (1.68 ± 0.11-fold; $n = 6$), or 30 nM thrombin (Fig. 7*B*). Low concentrations of thrombin (0.3–3 nM) that were capable of evoking PAR1-mediated potentiation of NMDA receptor function did not produce any cleavage of NR1 subunit (Fig. 3), further suggesting that the potentiation that we observed is independent of thrombin proteolysis of NR1.

To confirm that activation of PAR1 leads to NMDA receptor current potentiation, we tested whether the PAR1-activating peptide (10–30 μM SFLLRN) could potentiate recombinant NMDA receptor responses in oocytes coinjected with PAR1 cRNA. Oocytes expressing NR1–1a/NR2B NMDA receptor subunits but not PAR1 had a ratio of the NMDA receptor-mediated current after thrombin application to the current response before thrombin application of 0.87 ± 0.04 ($n = 9$). By contrast, oocytes expressing the same NMDA receptor subunits and PAR1 had a significantly larger ratio after SFLLRN stimulation of PAR1 (Fig. 7*A*) (1.41 ± 0.11-fold potentiation; $p < 0.01$; paired *t* test; $n = 9$). Similar results were found for SFLLRN potentiation of NR1–1a/NR2A receptors (1.85 ± 0.1-fold potentiation; $n = 6$). These data showing SFLLRN potentiation of recombinant NMDA receptor responses rule out the possibility that thrombin cleavage of substrates other than PAR1 might contribute to the observed NMDA receptor potentiation.

To evaluate the subunit dependence of PAR1 potentiation of NMDA receptor responses, we coinjected oocytes with various subunit combinations. Figure 7*C* shows several NR1 splice variants coexpressed with NR2B that were tested for their sensitivity to PAR1 potentiation of receptor function. The NR1–4aΔstop mutation eliminates 22 C-terminal amino acids included in the NR1–4a subunit as a result of a frame shift associated with the

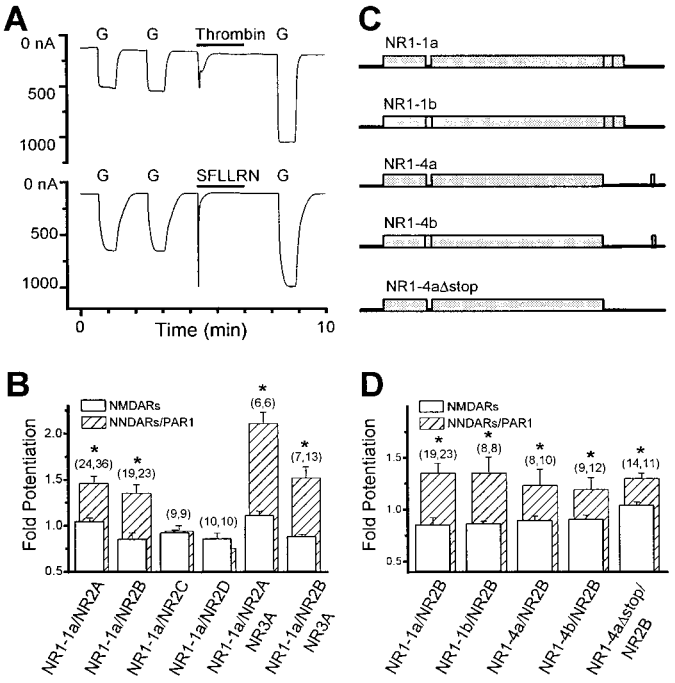

Figure 7. *A*, *Xenopus* oocytes were coinjected with NR1–1a/NR2B cRNAs or NR1–1a/NR2B/PAR1. Current recordings were made under voltage clamp at −30 mV in the nominal absence of extracellular Mg^{2+}. The current–response to 20 μM glutamate plus 10 μM glycine (*G* in *all panels*) was potentiated after activation of PAR1 by either 2.5 U/ml (25 nM) thrombin or 10 μM SFLLRN. Activation of PAR1 initiates an endogenous Ca^{2+}-activated Cl^- current; no such responses were evoked by thrombin treatment of oocytes that were not coinjected with PAR1 cRNA ($n = 127$; data not shown). *B*, Although thrombin (2.5 U/ml)-stimulated or SFLLRN (10–30 μM)-stimulated Ca^{2+}-activated Cl^- currents were observed in oocytes coinjected with PAR1 and NR1 plus NR2A, NR2B, NR2C, NR2D, or NR3A, only responses from NMDA receptors containing NR1 plus NR2A, NR2B, NR2A/NR3A, or NR2B/NR3A were potentiated by activation of PAR1 cDNA. *C*, Linear map showing alternative splice variants of the NR1 subunit that were studied. NR1–4aΔstop was created by mutation of the codon for Q866 in the NR1 cDNA to a stop codon. *D*, Alternative C- or N-terminal NR1 splicing or creation of a new reading frame by use of an alternative splice site within exon 22 does not markedly alter PAR1-mediated potentiation of NMDA receptor responses. For all panels, * indicates significantly different from oocytes without PAR1 coinjection ($p < 0.05$ by *t* test); number of oocytes indicated in *parentheses*. Data are mean ± SEM.

use of an alternative splice site in exon 22. Receptors containing all splice variants tested were significantly potentiated by PAR1 activation (Fig. 7*D*). The NR2 subunit had a more marked effect on PAR1 potentiation of NMDA receptor function. Oocytes coinjected with NR1–1a and either the NR2A or NR2B subunit were potentiated by thrombin activation of PAR1 (Fig. 7*B*). Coexpression of NR3A with NR1–1a/NR2A or NR1–1a/NR2B subunits did not occlude PAR1-mediated potentiation. However, the amplitude of NMDA receptor responses in oocytes coinjected with NR1–1a and either NR2C or NR2D was unaffected by thrombin activation of PAR1. These results suggest that only receptors that contain NR1/NR2A or NR1/NR2B subunits can be potentiated by PAR1 activation. In addition, these data are consistent with the idea that NR1 splicing alone does not dominate the molecular determinants of PAR1 potentiation in our Ba^{2+}-containing recording solution (Zheng et al., 1997; Logan et al., 1999).

The potentiation of recombinant NMDA receptor responses by thrombin activation of PAR1 was independent of voltage over the range −80 to +30 mV ($n = 6$; data not shown). The potentiation that we observed occurred for responses to maximal concentrations of glutamate and glycine, eliminating the possibility that potentiation reflects an increase in the glutamate or glycine EC_{50}. PAR1 potentiation could also be observed for NR1–1a(C798A)/NR2B receptors (1.35 ± 0.07-fold; $n = 7$; $p < 0.05$ by *t* test) compared with control oocytes lacking PAR1 (0.98 ± 0.05; $n = 5$), which rules out any contribution to the potentiation that we observed of changes in reduction/oxidation state of the disulfide linkage in NR1 (Sullivan et al., 1994). In addition, PAR1 potentiation of recombinant NMDA receptor responses does not significantly alter the ratio of current responses at pH 7.6 and pH 6.8 (Fig. 8*C*,*D*), suggesting that PAR1 activation does not relieve tonic proton inhibition (Traynelis and Cull-Candy, 1990). This result is consistent with the lack of effect (Fig. 7) of alternate splicing of NR1 exon 5 on PAR1 potentiation (Traynelis et al., 1995). Potentiation of NR2A-containing receptors was observed both in the absence (Fig. 7) and presence of 10 μM EDTA (2.01 ± 0.17-fold; $n = 12$), eliminating any contribution of PAR1-mediated relief of tonic inhibition by contaminant Zn^{2+} in our recording solutions (Paoletti et al., 1997; Zheng et al., 1998). Figure 8*A*,*B* shows that PAR1-mediated potentiation did not reduce Mg^{2+} block of recombinant NMDA receptors. The modest enhancement of Mg^{2+} blockade after thrombin activation of PAR1 for NR1–1a/NR2B/NR3A receptors was not significantly different from a modest enhancement of Mg^{2+} potentiation observed in thrombin-treated control oocytes that did not express PAR1 (data not shown; $n = 7$), suggesting that it was not linked to PAR1 activation.

Thrombin potentiation of neuronal NMDA receptor function is voltage dependent

Hippocampal NMDA receptors are under strong voltage-dependent block by extracellular Mg^{2+}, as illustrated by the current–voltage curve from hippocampal CA1 pyramidal cells shown in Figure 9*A*. To investigate whether the thrombin-induced potentiation of neuronal NMDA receptors is independent of voltage-dependent Mg^{2+} blockade, we compared the ratio of NMDA-evoked whole-cell currents recorded at −70 and −40 mV in control cells. We found that the ratio of current recorded at −70 to −40 mV was significantly larger after thrombin treatment when compared with pretreatment control ($n = 22$; Wilcoxon rank sum test; $p < 0.01$) (Fig. 9*B*). Moreover, in 16 of 21 CA1 pyramidal cells examined, the potentiation of NMDA receptor responses by thrombin was larger at −70 mV (Fig. 9*C*, *open symbols*). Average peak potentiation was 2.10 ± 0.29-fold at −70 mV and 1.48 ± 0.11-fold at −40 mV in 1.4 mM Mg^{2+} ($n = 19$; Wilcoxon rank sum test; $p < 0.01$) (Fig. 9*D*,*E*). Interestingly, the magnitude of potentiation observed at −40 mV was virtually identical to that observed in *Xenopus* oocytes in the absence of Mg^{2+} (Fig. 9*E*). We interpret these data to suggest that there may be an additional voltage-dependent component to the potentiation of neuronal NMDA receptors at hyperpolarized potentials after thrombin activation of PAR1 that is not present in *Xenopus* oocytes (Fig. 5) (Durand et al., 1993; Wagner and Leonard, 1996; Zheng et al., 1997; Xiong et al., 1998). One potential explanation of this result is that PAR1 activation modestly reduces the voltage-dependent Mg^{2+} block of neuronal NMDA receptors in addition to potentiating receptor function in a voltage-independent fashion. Two previous reports of PKC-mediated relief of Mg^{2+} blockade of neuronal NMDA receptor responses (Chen and Huang, 1992; Zhang et al., 1996) are consistent with

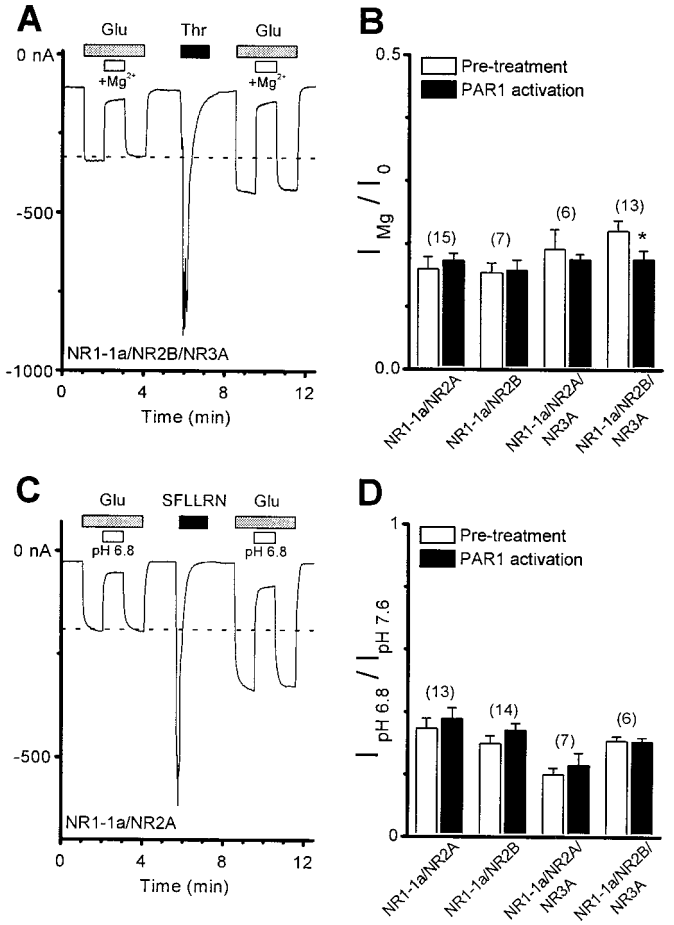

Figure 8. *A*, PAR1 activation by 3 U/ml of thrombin (*black bar*) potentiated glutamate-evoked NMDA receptor responses (*gray bars*) without altering inhibition by 0.2 mM Mg^{2+} (*open bars*). *B*, The effects of PAR1 activation on inhibition by Mg^{2+} are summarized for different combinations of NMDA receptor subunits. *Number* in *parentheses* indicates the number of oocytes. The mean inhibition by Mg^{2+} is shown and was calculated from each oocyte as the ratio of the glutamate/glycine-evoked current during Mg^{2+} application (I_{Mg}) to the pretreatment current (I_O). Data are mean ± SEM. All oocytes showed robust potentiation of NMDA receptors responses after PAR1 activation. *C*, PAR1 activation by the agonist peptide 10 μM SFLLRN (*black bar*) potentiated glutamate-evoked NMDA receptor responses (*gray bars*) without significantly altering inhibition produced by lowering pH from 7.6 (control) to 6.8 (*open bars*). *D*, The effects of PAR1 activation on proton inhibition are summarized for different combinations of NMDA receptor subunits. *Number* in *parentheses* indicates the number of oocytes. The mean inhibition by pH 6.8 is shown and was calculated from each oocyte as the ratio of the glutamate/glycine-evoked current at pH 6.8 ($I_{pH\ 6.8}$) to the pretreatment current ($I_{pH\ 7.6}$). Data are mean ± SEM. All oocytes showed robust potentiation of NMDA receptors responses after PAR1 activation. For all panels, * indicates $p < 0.05$ (*t* test).

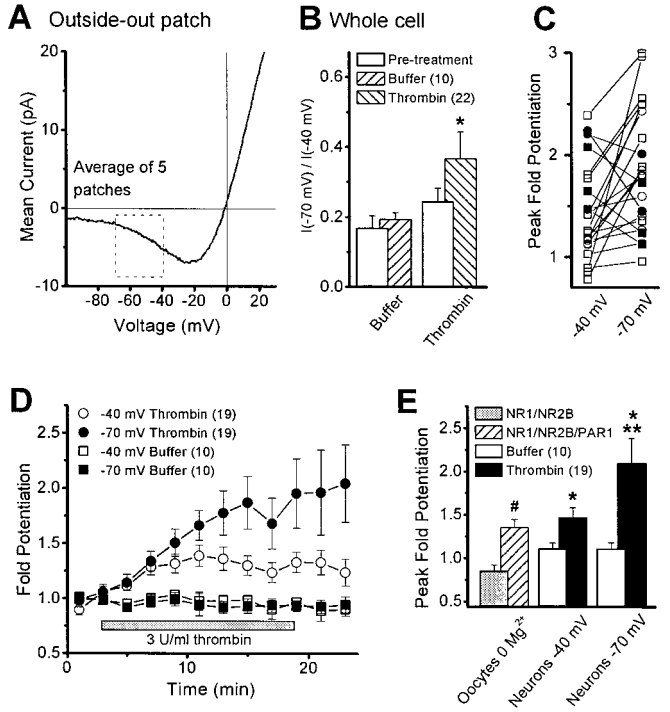

Figure 9. *A*, The mean current–voltage relationship from five outside-out patches excised from CA1 pyramidal cells in hippocampal slices. In each patch, the voltage was ramped between −100 and +30 mV (1–2 sec) between 10 and 50 times in the absence and presence of 50 μM NMDA plus 10 μM glycine. The resulting traces from each patch were averaged together and subtracted; data between patches were subsequently averaged. The *box* highlights the region analyzed in whole-cell recordings. *B*, The mean ratio (±SEM) of the whole-cell current–response to pressure-applied NMDA/glycine measured at −70 and at −40 mV is shown before (*Pre-treatment*) and after 20–30 min of thrombin or buffer treatment. * indicates significantly different from pretreatment ($p < 0.05$; Wilcoxon rank sum test). *C*, Plots show increased peak fold potentiation at −70 mV compared with −40 mV for most cells studied (*open symbols*); a few cells showed larger peak fold potentiation at −40 mV (*filled symbols*). *Squares* are data from rat, and *circles* are data from mouse. *D*, The time course (±SEM) of the fold potentiation recorded at both −70 and −40 mV in 19 cells in response to the application of 3 U/ml (30 nM) thrombin. *E*, The mean peak fold potentiation is shown after PAR1 activation for NR1–1a/NR2B receptors in *Xenopus* oocytes recorded in the absence of extracellular Mg^{2+}. Data are from Figure 7; # indicates $p < 0.05$ (*t* test). *Solid bars* show the mean peak fold potentiation for thrombin-treated hippocampal CA1 pyramidal cells, compared with ACSF-treated cells (*Buffer*). * indicates significantly different from buffer-treated cells ($p < 0.05$; Mann–Whitney test); ** indicates significantly different from neuronal results obtained at −40 mV ($p < 0.05$; Wilcoxon rank sum test).

this idea, because PAR1 is thought to couple to signaling systems linked to the G_O family of Gα-proteins, such as PKC (Grand et al., 1996). However, an alternative explanation for the voltage dependence of PAR1 potentiation of neuronal receptors is that PAR1-linked modification or thrombin proteolysis of other channels or membrane proteins reduces our ability to keep the dendrites under voltage control. The resulting reduction in holding potential of distal dendrites during NMDA receptor activation might modestly reduce NMDA receptor block by extracellular Mg^{2+}, causing an apparent supplemental potentiation of the NMDA receptor response. Although we can detect no thrombin-induced changes in membrane resistance and have blocked some K^+, Na^+, and Ca^{2+} channels with Cs^+, QX-314, and nifedipine, the complex electrotonic structure of CA1 hippocampal pyramidal cells makes it difficult to dismiss this alternative possibility. Ultimately, single-channel studies in which individual Mg^{2+}-induced blockages of the NMDA receptor are evaluated will be required to assess whether PAR1 activation also causes any reduction of Mg^{2+} blockade.

DISCUSSION

In this study we have demonstrated under multiple experimental paradigms that the serine protease thrombin at nanomolar concentrations can potentiate recombinant and hippocampal NMDA receptor function. The potentiation of neuronal NMDA receptor responses appears to reflect activation of the Gα-protein-coupled

protease receptor PAR1, which is differentially expressed throughout the CNS. Although high concentrations of thrombin can directly cleave the hippocampal NR1 subunit, multiple lines of evidence suggest that the PAR1-mediated potentiation that we observed is independent of NMDA receptor proteolysis. These results hold intriguing implications for both neuronal development and neuropathological situations in which compromise of the blood–brain barrier provides access for blood-derived serine proteases that are capable of activating PAR1 to brain parenchyma. Furthermore, these results raise the possibility that expression of thrombin by neural tissue (Dihanich et al., 1991) might act on PAR1 to influence NMDA receptor function.

PAR1 potentiation of NMDA receptors in normal brain function

The control of NMDA receptor function by serine proteases may play a role in normal brain function, given the important contribution to synaptic plasticity and neuronal development suggested for NMDA receptors. A role for the serine proteases tPA in late-phase long-term potentiation of excitatory synaptic function has recently been suggested (Baranes et al., 1998; Zhuo et al., 2000), and our results raise the possibility that PAR1 activation might influence the contribution of NMDA receptor activation to various forms of synaptic plasticity. PAR1 has been suggested to play a role in neuronal development on the basis of thrombin's stimulation of neurite retraction (Gurwitz and Cunningham, 1988) and reversal of astrocyte stellation (Grabham and Cunningham, 1995). The ability of thrombin and other serine proteases such as plasmin (Junge et al., 1999) to potentiate NMDA receptor function and thus enhance Ca^{2+} signaling could be important for several developmental processes that are influenced by NMDA receptors, including synapse stabilization (Scheetz and Constantine-Paton, 1994), neuronal survival (Ikonomidou et al., 1999), neuronal migration (Komuro and Rakic, 1993), as well as growth cone guidance (Baird et al., 1996; Zheng et al., 1996). Several additional studies provide support for serine protease and PAR1 involvement in synaptic (Liu et al., 1994; Baranes et al., 1998) and neuronal development (Debeir et al., 1998). Thus, our results are consistent with a number of potential roles of serine protease signaling in the CNS.

PAR1 potentiation of NMDA receptor function in pathological situations

It is now well accepted that NMDA receptor overactivation plays a role in expanding the region of neuronal injury after experimental ischemia (Whetsell, 1996; Dirnagl et al., 1999; Lee et al., 1999). Thus, it is possible that thrombin entry into the brain during hemorrhagic stroke and penetrating head wound may contribute to neuronal damage through potentiation of NMDA receptor function. If thrombin is generated in sufficient quantities to enter brain tissue in excess of endogenous serine protease inhibitors such as PN-1 (Luthi et al., 1997) during other cardiovascular insults that compromise blood–brain barrier integrity (e.g., occlusive stroke, closed head injury, status epilepticus) (Laursen et al. 1993; Barzo et al., 1997; Correale et al., 1998), thrombin might contribute to the neuropathology of these conditions through potentiation of NMDA receptors. Similarly, if other serine proteases capable of activating brain PARs such as plasmin (Ishihara et al., 1997) also potentiate NMDA receptor function (Junge et al., 1999), they too may have harmful effects should they reach brain parenchyma. Extravasated plasminogen has been suggested to be cleaved by tPA in brain tissue to produce abnormally high levels of plasmin, which may be important for neuronal damage after experimental ischemia or injection of kainic acid (Tsirka et al., 1995, 1997a,b; Wang et al., 1998; Kim et al., 1999). The effects of serine proteases and their receptors on neuronal function is a timely topic given the current use of the protease tPA in treatment of occlusive stroke (Hacke et al., 1995; Wardlaw et al., 1997).

The recent demonstration that thrombin entry into the brain can evoke seizures (Lee et al., 1997) together with the thrombin-mediated potentiation of NMDA receptor responses described here suggests that thrombin together with heme-derived iron (Willmore et al., 1978) could be a contributing factor to post-traumatic seizures. Unprovoked seizures complicate 7–34% of civilian and combat trauma patients, and 2–25% of patients with cerebrovascular disease or intracerebral bleeding suffer seizures, with a higher incidence in hemorrhagic than ischemic stroke (Berger et al., 1988; Faught et al., 1989; Lancman et al., 1993; Arboix et al., 1997). Interestingly, the best indicators of post-traumatic epilepsy include subdural hematoma and intracerebral hemorrhage, two conditions that should lead to thrombin entry into the brain (Lee and Lui, 1992; Annegers et al., 1998). Our data showing thrombin potentiation of NMDA receptor function plus plasmin-induced reductions in GABAergic transmission (Mizutani et al., 1997) are consistent with the idea that serine proteases can control neuronal excitability (Luthi et al., 1997). Thus, although more work is needed to elucidate the details of protease signaling in the brain, our results strengthen the idea that serine proteases and their receptors have important roles in both normal and pathological situations.

Comparison of results with previous work

The PAR1-induced potentiation of neuronal NMDA receptor function that we observed at −40 mV is similar to potentiation of neuronal NMDA receptors after activation of various G-protein-linked receptor systems, including m1 muscarinic receptors (Markram and Segal, 1990; Marino et al., 1998), metabotropic glutamate receptors (mGluRs) (Aniksztejn et al., 1991, 1992), and μ opioid receptors (Chen and Huang, 1991). In addition, the PAR1-mediated potentiation of recombinant NMDA receptor responses in *Xenopus* oocytes is similar to 5-HT_2 and mGluR receptor potentiation of recombinant NMDA receptors (Kelso et al., 1992; Blank et al., 1996). The potentiation of NMDA receptor function after activation of mGluRs, 5-HT_2 receptors, and μ opioid receptors has been suggested to require PKC (Aniksztejn et al., 1991, 1992; Chen and Huang, 1991; Kelso et al., 1992; Blank et al., 1996). Furthermore, purified PKC can potentiate (Chen and Huang, 1991, 1992; Xiong et al., 1998) as well as phosphorylate NMDA receptors (Tingley et al., 1993, 1997; Leonard and Hell, 1997). Moreover, the NR2 subunit dependence of PAR1 potentiation is consistent with the subunit dependence of phorbol ester potentiation of heteromeric NMDA receptor function in oocytes (Kutsuwada et al., 1992; Mori et al., 1993; Grant et al., 1998). These findings, together with the coupling of PAR1 receptors to the G_O family of Gα-proteins, which can lead to PKC activation, make PKC an attractive candidate pathway for PAR1 potentiation of neuronal NMDA receptor responses. Our data showing that the protein kinase inhibitor BIS can block PAR1 potentiation of neuronal NMDA responses are also suggestive of a role for PKC, although we cannot rule out involvement of other serine/threonine kinases because the concentration of BIS used to ensure penetration into the slice was nonselective. Moreover, it is possible that other signaling systems that couple to PAR1 (Dery

et al., 1998), G_O and G_I family of Gα-proteins (Bence et al., 1997; Umemori et al., 1997), or PKC (Le Good et al., 1998; Marais et al., 1998) might mediate the effects of PAR1 on NMDA receptor function. Furthermore, kinase regulation of the binding of intracellular proteins to glutamate receptors (Matsuda et al., 1999) raises another level of potential complexity to the signaling that we observed. Thus, more work is required to elucidate the pathway(s) underlying PAR1 potentiation of NMDA receptor function.

REFERENCES

Andrew RD, MacVicar BA (1994) Imaging cell volume changes and neuronal excitation in the hippocampal slice. Neuroscience 62:371–383.

Aniksztejn L, Bregestovski P, Ben-Ari Y (1991) Selective activation of quisqualate metabotropic receptor potentiates NMDA but not AMPA responses. Eur J Pharmacol 205:327–328.

Aniksztejn L, Otani S, Ben-Ari Y (1992) Quisqualate metabotropic receptors modulate NMDA currents and facilitate induction of long term potentiation through protein kinase C. Eur J Neurosci 4:500–505.

Annegers JF, Hauser WA, Coan SP, Rocca WA (1998) A population-based study of seizures after traumatic brain injuries. N Engl J Med 338:20–24.

Arand AG, Sawaya R (1986) Intraoperative chemical hemostasis in neurosurgery. Neurosurgery 18:223–233.

Arboix A, Garcia-Eroles L, Massons JB, Oliveres M, Comes E (1997) Predictive factors of early seizures after acute cerebrovascular disease. Stroke 28:1590–1594.

Baird DH, Trenkner E, Mason CA (1996) Arrest of afferent axon extension by target neurons *in vitro* is regulated by the NMDA receptor. J Neurosci 16:2642–2648.

Baranes D, Lederfein D, Huang YY, Chen M, Bailey CH, Kandel ER (1998) Tissue plasminogen activator contributes to the late phase of LTP and to synaptic growth in the hippocampal mossy fiber pathway. Neuron 21:813–825.

Barzo P, Marmarou A, Fatouros P, Corwin F, Dunbar JG (1997) Acute blood-brain barrier changes in experimental closed head injury as measured by MRI and Gd-DTPA. Acta Neurochir Suppl (Wien) 70:243–246.

Bence K, Ma W, Kozasa T, Huang X-Y (1997) Direct stimulation of Bruton's tyrosine kinase by G_O-protein α-subunit. Nature 389:296–299.

Berger AR, Lipton RB, Lesser ML, Lantos G, Portenoy RK (1988) Early seizures following intracerebral hemorrhage: implication for therapy. Neurology 38:1363–1365.

Blank T, Zwart R, Nijholt I, Spiess J (1996) Serotonin 5-HT2 receptor activation potentiates *N*-methyl-D-aspartate receptor-mediated ion currents by a protein kinase C-dependent mechanism. J Neurochem Res 45:153–160.

Bradford HF (1995) Glutamate, GABA, and epilepsy. Prog Neurobiol 47:477–511.

Butler MA, Traynelis SF (1996) Native and recombinant NMDA receptors are cleaved by the serine protease thrombin. Soc Neurosci Abstr 22:1761.

Cavanaugh KP, Gurwitz D, Cunningham DD, Bradshaw RA (1990) Reciprocal modulation of astrocyte stellation by thrombin and protease nexin-1. J Neurochem 54:1735–1743.

Chen C, Okayama H (1987) High-efficiency transformation of mammalian cells by plasmid DNA. Mol Cell Biol 7:2745–2752.

Chen L, Huang L-YM (1991) Sustained potentiation of NMDA receptor-mediated glutamate responses through activation of protein kinase C by a μ opioid. Neuron 7:319–326.

Chen L, Huang L-Y (1992) Protein kinase C reduces Mg^{2+} block of NMDA receptor channels as a mechanism of modulation. Nature 356:521–523.

Chen Z-L, Yoshida S, Kato K, Momota Y, Suzuki J, Tanaka T, Ito J, Nishino H, Aimoto S, Kiyama H, Shiosaka S (1995) Expression and activity-dependent changes of a novel limbic-serine protease gene in the hippocampus. J Neurosci 15:5088–5097.

Connolly AJ, Ishihara H, Kahn ML, Farese RV, Coughlin SR (1996) Role of the thrombin receptor in development and evidence for a second receptor. Nature 381:516–519.

Correale J, Rabinowicz AL, Heck CN, Smith TD, Loskota WJ, DeGiorgio CM (1998) Status epilepticus increases CSF levels of neuron-specific enolase and alters the blood brain barrier. Neurology 50:1388–1391.

Debeir T, Benavides J, Vige X (1998) Involvement of protease activated receptor-1 in the *in vitro* development of mesencephalic dopaminergic neurons. Neuroscience 82:739–752.

Dery O, Corver CU, Steinhoff M, Bunnett NW (1998) Proteinase-activated receptors: novel mechanisms of signaling by serine proteases. Am J Physiol 274:C1429–C1452.

Dihanich M, Kaser M, Reinhard E, Cunningham DD, Monard D (1991) Prothrombin mRNA is expressed by cells of the nervous system. Neuron 6:575–581.

Dirnagl U, Iadecola C, Moskowitz MA (1999) Pathobiology of ischaemic stroke: an integrated view. Trends Neurosci 22:391–397.

Donovan FM, Pike CJ, Cotman CW, Cunningham DD (1997) Thrombin induces apoptosis in cultured neurons and astrocytes via a pathway requiring tyrosine kinase and RhoA activities. J Neurosci 17:5316–5326.

Du C, Hu R, Hsu CY, Choi DW (1996) Dextrorphan reduces infarct volume, vascular injury, and brain edema after ischemic brain injury. J Neurotrauma 13:215–222.

Durand GM, Bennett MV, Zukin RS (1993) Splice variants of the *N*-methyl-D-aspartate receptor NR1 identify domains involved in regulation by polyamines and protein kinase C. Proc Natl Acad Sci USA 90:6731–6735.

Faught E, Peters D, Bartolucci A, Moore L, Miller PC (1989) Seizures after primary intracerebral hemorrhage. Neurology 39:1089–1093.

Gerszten RE, Chen J, Ishii M, Ishii K, Wang L, Nanevicz T, Turck CW, Vu T-KH, Coughlin SR (1994) Specificity of the thrombin receptor for agonist peptide is defined by its extracellular surface. Nature 368:648–651.

Gingrich MB, Traynelis SF (1998) Protease activated receptor-1 potentiation of NMDA receptor function is Mg^{++} dependent. Soc Neurosci Abstr 24:1271.

Gingrich MB, Ciliax NF, Traynelis SF (1997) Thrombin treatment of cultured hippocampal neurons attenuates Mg^{2+} block of the NMDA receptor. Soc Neurosci Abstr 23:947.

Gingrich MB, Rouse ST, Marino MJ, Conn PJ, Traynelis SF (1998) Potentiation of neuronal and recombinant NMDA receptors by activation of the thrombin receptor PAR1 in *Xenopus* oocytes and rat hippocampal slices. J Physiol (Lond) 507:26P.

Grabham P, Cunningham DD (1995) Thrombin receptor activation stimulates astrocyte proliferation and reversal of stellation by distinct pathways: involvement of tyrosine phosphorylation. J Neurochem 64:583–591.

Grand RJ, Turnell AS, Grabham P (1996) Cellular consequences of thrombin-receptor activation. Biochem J 313:353–368.

Grant ER, Bacskai BJ, Anegawa NJ, Pleasure DE, Lynch DR (1998) Opposing contributions of NR1 and NR2 to protein kinase C modulation of NMDA receptors. J Neurochem 71:1471–1481.

Gschwend TP, Krueger SR, Kozlov SV, Wolfer DP, Sonderegger P (1997) Neurotrypsin, a novel multidomain serine protease expressed in the central nervous system. Mol Cell Neurosci 9:207–219.

Gurwitz D, Cunningham DD (1988) Thrombin modulates and reverses neuroblastoma neurite outgrowth. Proc Natl Acad Sci USA 85:3440–3444.

Hacke W, Kaste M, Fieschi C, Toni D, Lesaffre E (1995) Intravenous thrombolysis with recombinant tissue plasminogen activator for acute hemispheric stroke: the European cooperative acute stroke study (ECASS). JAMA 274:1017–1025.

Hall KE, Browning MD, Dudek EM, MacDonald RL (1995) Enhancement of high threshold calcium currents in rat primary afferent neurons by constitutively active protein kinase C. J Neurosci 15:6069–6076.

Hastings GA, Coleman TA, Haudenschild CC, Stefansson S, Smith EP, Barthlow R, Cherry S, Sandkvist M, Lawrence DA (1997) Neuroserpin, a brain-associated inhibitor of tissue plasminogen activator is localized primarily in neurons: implications for the regulation of motor learning and neuronal survival. J Biol Chem 272:33062–33067.

Ikonomidou C, Bosch F, Miksa M, Bittigau P, Vockler J, Dikranian K, Tenkova TI, Stefovska V, Turski L, Olney JW (1999) Blockade of NMDA receptors and apoptotic neurodegeneration in the developing brain. Science 283:70–74.

Ishihara H, Connolly AJ, Zeng D, Kahn ML, Zhent YW, Timmons C,

Tram T, Coughlin SR (1997) Protease-activated receptor 3 is a second thrombin receptor in humans. Nature 386:502–506.

Junge C, Mannaioni G, Gingrich MB, Traynelis SF (1999) Plasmin and thrombin regulation of NMDA receptor function. Soc Neurosci Abstr 25:1979.

Kelso SR, Nelson TE, Leonard JP (1992) Protein kinase C-mediated enhancement of NMDA currents by metabotropic glutamate receptors in *Xenopus* oocytes. J Physiol (Lond) 449:705–718.

Kim Y-H, Park J-H, Hong SH, Koh J-Y (1999) Nonproteolytic neuroprotection by human recombinant tissue plasminogen activator. Science 284:647–650.

Komuro H, Rakic P (1993) Modulation of neuronal migration by NMDA receptors. Science 260:95–97.

Krueger SR, Ghisu G-P, Cinelli P, Gschwend TP, Osterwalder T, Wolfer DP, Sonderegger P (1997) Expression of neuroserpin, an inhibitor of tissue plasminogen activator, in developing and adult nervous system of the mouse. J Neurosci 17:8984–8996.

Kutsuwada T, Kashiwabuchi N, Mori H, Sakimura K, Kushiya E, Araki K, Meguro H, Masaki H, Kumanishi T, Arakawa M, Mishina M (1992) Molecular diversity of the NMDA receptor channel. Nature 358:36–41.

Lancman ME, Golimstok A, Norscini J, Granillo R (1993) Risk factors for developing seizures after a stroke. Epilepsia 34:141–143.

Lau L-F, Huganir RL (1995) Differential tyrosine phosphorylation of *N*-methyl-D-aspartate receptor subunits. J Biol Chem 270:20036–20041.

Laursen H, Hansen AJ, Sheardown M (1993) Cerebrovascular permeability and brain edema after photochemical infarcts in the rat. Acta Neuropathol (Berl) 86:378–385.

Lee J-M, Zipfel GJ, Choi DW (1999) The changing landscape of ischaemic brain injury mechanisms. Nature 399[Suppl]:A7–A14.

Lee KR, Colon GP, Betz AL, Keep RF, Kim S, Hoff JT (1996) Edema from intracerebral hemorrhage: the role of thrombin. J Neurosurg 84:91–96.

Lee KR, Drury I, Vitarbo E, Hoff JT (1997) Seizures induced by intracerebral injection of thrombin: a model of intracerebral hemorrhage. J Neurosurg 87:73–78.

Lee S-T, Lui T-N (1992) Early seizures after mild closed head injury. J Neurosurg 76:435–439.

Le Good JA, Ziegler WH, Parekh DB, Alessi DR, Cohen P, Parker PJ (1998) Protein kinase C isotypes controlled by phosphoinositide 3-kinase through protein kinase PDK1. Science 281:2042–2045.

Leonard AS, Hell JW (1997) Cyclic AMP-dependent protein kinase and protein kinase C phosphorylate *N*-methyl-D-aspartate receptors at different sites. J Biol Chem 272:12107–12115.

Liu Y, Fields RD, Festoff BW, Nelson PG (1994) Proteolytic action of thrombin is required for electrical activity-dependent synapse reduction. Proc Natl Acad Sci USA 91:10300–10304.

Logan SM, Rivera FE, Leonard JP (1999) Protein kinase C modulation of recombinant NMDA receptor currents: roles for the C-terminal C1 exon and calcium ions. J Neurosci 19:974–986.

Luthi A, van der Putten H, Botteri FM, Mansuy IM, Meins M, Frey U, Sansig G, Portet C, Schmutz M, Schroder M, Nitsch C, Laurent J-P, Monard D (1997) Endogenous serine protease inhibitor modulates epileptic activity and hippocampal long-term potentiation. J Neurosci 17:4688–4699.

Majerus PW, Broze GJ, Miletich JP, Tollefsen DM (1996) Anticoagulant, thrombolytic, and antiplatelet drugs. In: Goodman & Gilman's the pharmacological basis of therapeutics, Ed 9 (Hardman JG, Limbird LE, eds), p 1351. New York: McGraw-Hill.

Marais R, Light Y, Mason C, Paterson H, Olson MF, Marshall CJ (1998) Requirement of Ras-GTP-Raf complexes for activation of Raf-1 by protein kinase C. Science 280:109–112.

Marino MJ, Rouse ST, Levey AI, Potter LT, Conn PJ (1998) Activation of the genetically defined m1 muscarinic receptor potentiates *N*-methyl-D-aspartate (NMDA) receptor currents in hippocampal pyramidal cells. Proc Natl Acad Sci USA 95:11465–11470.

Markram H, Segal M (1990) Long-lasting facilitation of excitatory postsynaptic potentials in the rat hippocampus by acetylcholine. J Physiol (Lond) 427:381–393.

Matsuda S, Mikawa S, Hirai H (1999) Phosphorylation of serine-880 in GluR2 by protein kinase C prevents its C terminus from binding with glutamate receptor interacting protein. J Neurochem 73:1765–1768.

McBain CJ, Traynelis SF, Dingledine R (1990) Regional variation of extracellular space in hippocampus. Science 249:674–677.

Miledi R (1982) A calcium-dependent transient outward current in *Xenopus laevis* oocytes. Proc R Soc Lond B Biol Sci 215:491–497.

Miledi R, Parker I (1984) Chloride current induced by injection of calcium into *Xenopus* oocytes. J Physiol (Lond) 357:173–183.

Mizutani A, Tanaka T, Saito H, Matsuki N (1997) Postsynaptic blockade of inhibitory postsynaptic currents by plasmin in CA1 pyramidal cells of rat hippocampal slices. Brain Res 761:93–96.

Mori H, Yamakura T, Masaki H, Mishina M (1993) Involvement of the carboxy-terminal region in modulation by TPA of the NMDA receptor channel. NeuroReport 4:519–522.

Motohashi O, Suzuki M, Shida N, Umezawa K, Sugai K, Yoshimoto T (1997) Hirudin suppresses the invasion of inflammatory cells and the appearance of vimentin-positive astrocytes in the rat cerebral ablation model. J Neurotrauma 14:747–754.

Nagy Z, Kolev K, Csonka E, Vastag M, Machovich R (1998) Perturbation of the integrity of the blood brain barrier by fibrinolytic enzymes. Blood Coagul Fibrinolysis 9:471–478.

Nakajima K, Tsuzaki N, Nagata K, Takemoto N, Kohsaka S (1992) Production and secretion of plasminogen in cultured rat brain microglia. FEBS Lett 308:179–182.

Niclou SP, Suidan HS, Pavlik A, Vejsada R, Monard D (1998) Changes in the expression of protease-activated receptor 1 and protease nexin-1 mRNA during rat nervous system development and after nerve lesion. Eur J Neurosci 10:1590–1607.

Nishino A, Suzuki M, Ohtani H, Motohashi O, Umezawa K, Nagura H, Yoshimoto T (1993) Thrombin may contribute to the pathophysiology of central nervous system injury. J Neurotrauma 10:167–179.

Obrenovitch TP, Urenjak J (1997) Is high extracellular glutamate the key to excitotoxicity in traumatic brain injury. J Neurotrauma 14:677–698.

Paoletti P, Ascher P, Neyton J (1997) High-affinity zinc inhibition of NMDA NR1-NR2A receptors. J Neurosci 17:5711–5725.

Pindon A, Hantai D, Jandrot-Perrus M, Festoff BW (1997) Novel expression and localization of active thrombomodulin on the surface of mouse brain astrocytes. Glia 19:259–268.

Sah P, Hestrin S, Nicoll RA (1989) Tonic activation of NMDA receptors by ambient glutamate enhances excitability of neurons. Science 246:815–818.

Scarisbrick IA, Towner MD, Isackson PJ (1997) Nervous system-specific expression of a novel serine protease regulation in the adult rat spinal cord by excitotoxic injury. J Neurosci 17:8156–8168.

Scheetz AJ, Constantine-Paton M (1994) Modulation of NMDA receptor function: implications for vertebrate neural development. FASEB J 8:745–752.

Seegers WH (1962) Prothrombin. Cambridge, MA: Harvard UP.

Shimizu C, Yoshida S, Shibata M, Kato K, Momota Y, Matsumoto K, Shiosaka T, Midorikawa R, Kamachi T, Kawabe A, Shiosaka S (1998) Characterization of recombinant and brain neuropsin, a plasticity-related serine protease. J Biol Chem 273:11189–11196.

Siegel SJ, Brose N, Janssen WG, Gasic GP, Jahn R, Heinemann SF, Morrison JH (1994) Regional, cellular, and ultrastructural distribution of *N*-methyl-D-aspartate receptor subunit 1 in monkey hippocampus. Proc Natl Acad Sci USA 91:564–568.

Sullivan JM, Traynelis SF, Chen H-SV, Escobar W, Heinemann SF, Lipton SA (1994) Identification of two cysteine residues that are required for redox modulation of the NMDA subtype of glutamate receptor. Neuron 13:929–936.

Sumi Y, Dent MA, Owen DE, Seeley PJ, Morris RJ (1992) The expression of tissue and urokinase-type plasminogen activators in neural development suggests different modes of proteolytic involvement in neuronal growth. Development 116:625–637.

Tapparelli C, Metternich R, Ehrhardt C, Cook NS (1993) Synthetic low-molecular weight thrombin inhibitors: molecular design and pharmacological profile. Trends Pharmacol Sci 14:366–376.

Tingley WG, Roche KW, Thompson AK, Huganir RL (1993) Regulation of NMDA receptor phosphorylation by alternative splicing of the C-terminal domain. Nature 364:70–73.

Tingley WG, Ehlers MD, Kameyama K, Doherty C, Ptak JB, Riley CT, Huganir RL (1997) Characterization of protein kinase A and protein kinase C phosphorylation of the *N*-methyl-D-aspartate receptor NR1 subunit using phosphorylation site specific antibodies. J Biol Chem 272:5157–5166.

Traynelis SF, Cull-Candy SG (1990) Proton inhibition of *N*-methyl-D-aspartate receptors in cerebellar neurons. Nature 345:347–350.

Traynelis SF, Hartley M, Heinemann SF (1995) Control of proton sensitivity of the NMDA receptor by RNA splicing and polyamines. Science 268:873–876.

Tsirka SE, Gualandris A, Amaral DG, Strickland S (1995) Excitotoxin-induced neuronal degeneration and seizure are mediated by tissue plasminogen activator. Nature 377:340–344.

Tsirka SE, Bugge TH, Degen JL, Strickland S (1997a) Neuronal death in the central nervous system demonstrates a non-fibrin substrate for plasmin. Proc Natl Acad Sci USA 94:9779–9781.

Tsirka SE, Rogove AD, Bugge TH, Degen JL, Strickland S (1997b) An extracellular proteolytic cascade promotes neuronal degeneration in the mouse hippocampus. J Neurosci 17:543–552.

Umemori H, Inoue T, Kume S, Sekiyama N, Nagao M, Itoh H, Nakanishi S, Mikoshiba K, Yamamoto T (1997) Activation of the G protein Gq/11 through tyrosine phosphorylation of the α subunit. Science 276:1878–1881.

Vu T-KH, Hung DT, Wheaton VI, Coughlin SR (1991) Molecular cloning of a functional thrombin receptor reveals a novel proteolytic mechanism of receptor activation. Cell 64:1057–1068.

Wagner DA, Leonard JP (1996) Effect of protein kinase C activation of the Mg^{2+} sensitivity of cloned NMDA receptors. Neuropharmacology 35:29–36.

Wang YF, Tsirka SE, Strickland S, Stieg PE, Soriano SG, Lipton SA (1998) Tissue plasminogen activator (tPA) increases neuronal damage after focal cerebral ischemia in wild-type and tPA-deficient mice. Nat Med 4:228–231.

Wardlaw JM, Warlow CP, Counsell C (1997) Systematic review of evidence on thrombolytic therapy for acute ischaemic stroke. Lancet 350:607–614.

Weinstein JR, Gold SJ, Cunningham DD, Gall CM (1995) Cellular localization of thrombin receptor mRNA in rat brain: expression by mesencephalic dopaminergic neurons and codistribution with prothrombin mRNA. J Neurosci 15:2906–2919.

Whetsell WO (1996) Current concepts of excitotoxicity. J Neuropathol Exp Neurol 55:1–13.

Willmore LJ (1990) Post-traumatic epilepsy: cellular mechanisms and implications for treatment. Epilepsia 31:[Suppl 3]:S67–S73.

Willmore LJ, Sypert GW, Munson JB, Hurd RW (1978) Chronic focal epileptiform discharge induced by injection of iron into rat and cat cortex. Science 200:1501–1503.

Xiong Z-G, Rauof R, Lu W-Y, Wang L-Y, Orser BA, Dudek EM, Browning MD, MacDonald JF (1998) Regulation of *N*-methyl-D-aspartate receptor function by constitutively active protein kinase C. Mol Pharmacol 54:1055–1063.

Yamada T, Nagai Y (1996) Immunohistochemical studies of human tissues with antibody to factor Xa. Histochem J 28:73–77.

Yamamoto K, Loskutoff DJ (1998) Extrahepatic expression and regulation of protein C in the mouse. Am J Pathol 153:547–555.

Yang Y, Akiyama H, Fenton JW, Brewer GJ (1997) Thrombin receptor on rat primary hippocampal neurons: coupled calcium and cAMP responses. Brain Res 761:11–18.

Zhang L, Rzigalinski BA, Ellis EF, Satin LS (1996) Reduction of voltage-dependent Mg^{2+} blockade of NMDA current in mechanically injured neurons. Science 274:1921–1923.

Zheng F, Gingrich MB, Traynelis SF, Conn PJ (1998) Tyrosine kinase potentiates NMDA receptor currents by reducing tonic zinc inhibition. Nat Neurosci 1:185–191.

Zheng JQ, Wan JJ, Poo MM (1996) Essential role of filopodia in chemotropic turning of nerve growth cone induced by a glutamate gradient. J Neurosci 16:1140–1149.

Zheng X, Zhang L, Wang AP, Bennett MVL, Zukin RS (1997) Ca^{2+} influx amplifies protein kinase C potentiation of recombinant NMDA receptors. J Neurosci 15:8676–8686.

Zhuo M, Holtzman DM, Li Y, Osaka H, DeMaro J, Jacquin M, Bu G (2000) Role of tissue plasminogen activator receptor LRP in hippocampal long-term potentiation. J Neurosci 20:542–549.